Glycobiology and Extracellular Matrices:

Binding of a sialic acid-recognizing lectin Siglec-9 modulates adhesion dynamics of cancer cells via calpain-mediated protein degradation

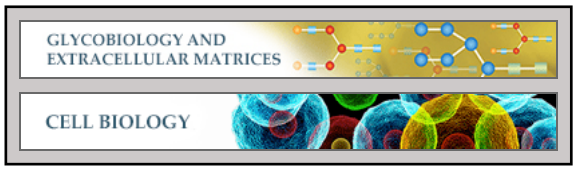

Ilhamjan Sabit, Noboru Hashimoto, Yasuyuki Matsumoto, Toshiyuki Yamaji, Keiko Furukawa and Koichi Furukawa

J. Biol. Chem. published online October 21, 2013

Binding of a sialic acid-recognizing lectin Siglec-9 modulates adhesion dynamics of cancer cells via calpain-mediated protein degradation

Ilhamjan Sabit[1], Noboru Hashimoto[1], Yasuyuki Matsumoto[1], Toshiyuki Yamaji[2], Keiko Furukawa[1,3], and Koichi Furukawa[1*]

[1]Department of Biochemistry II, Nagoya University Graduate School of Medicine, Nagoya 466-0065, Department of Biochemistry, [2]Department of Biochemistry and Cell Biology, National Institute of Infectious Diseases, Tokyo 162-8640, and [3]Department of Biomedical Sciences, Chubu University College of Life and Health Sciences, Kasugai 487-8501, Japan

Running title: *Siglec-9 modulates adhesion dynamics via calpain*

[*]To whom correspondence should be addressed: Koichi Furukawa, 65 Tsurumai, Showa-ku, Nagoya 466-0065, Japan. Tel: 81-52-744-2070; Fax: 81-52-744-2069; E-mail: koichi@med.nagoya-u.ac.jp

Background: Siglec-9 binds sialylglyco-conjugates on target cells probably causing signals in both sides of cells.

Results: Co-culture with Siglec-9-expressing U937 caused degradation of focal adhesion kinase and related proteins in an astrocytoma cell line.

Conclusion: Interaction between Siglec-9 and its counter receptor triggered activation signals in cancer cells via calpain.

Significance: Cancer cells may utilize sialylglycoconjugates recognized by Siglec-9 to escape from immunosurveillance.

Keywords: lectin; adhesion; protein degradation; sialic acid; calpain; focal adhesion kinase

SUMMARY

Although regulatory mechanisms for immune cells with inhibitory signals via immunoreceptor tyrosine-based inhibitory motifs (ITIM) have been well known, signals transduced via interaction between Siglecs and sialyl-compounds on their counter receptors into target cells are not reported to date. In this study, we found that an astrocytoma cell line, AS showed detachment from culture plates when co-cultured with Siglec-9-expressing cells and/or soluble Siglec-9. Moreover, detached AS cells re-grew as co-cultured cells with Siglec-9-deficient cells. They also showed increased motility and invasiveness upon Siglec-9 binding. In immunoblotting, rapid degradation of focal adhesion kinase (FAK) and related signaling molecules such as Akt, paxillin and p130Cas was observed immediately after the co-culture. Despite of degradation of these molecules, increased p-Akt was found at the front region of cytoplasm, probably reflecting increased cell motility. Calpain was considered to be a responsible protease for the protein degradation by the inhibition experiments. These results suggest that protein degradation of FAK and related molecules was induced by Siglec-9 binding to its counter receptors via sialylglycoconjugates, leading to the modulation of adhesion kinetics of cancer cells. Thus, this might be a mechanism by which cancer cells utilize Siglec-9-derived signals to escape from

immuno- surveillance.

Sialic acids are present as terminal monosaccharides linked to cell surface glycoconjugates, and play roles in a variety of physiological and pathological events (1). They are often a part of recognition sites for extrinsic pathogens (2). But they also play important roles by interacting with many intrinsic molecules, endogenous lectins. In particular, sialic acid-binding immunoglobulin-like lectins (Siglecs) are unique endogenous lectins recognizing sialic acid-containing carbohydrates on glycoproteins and glycosphingolipids (3). There are currently 14 known Siglecs in humans and 9 in mice, and majority of them are expressed on immune cells except Siglec-2 (3). One of the intriguing findings about Siglecs is that many of them have intracellular domains containing immunoreceptor tyrosine-based inhibitory motifs (ITIM), and exert as inhibitory receptors to negatively control the immune cells (3).

Siglecs have been thought to regulate the functions of innate immune cells and adaptive immune systems based on glycan recognition. In particular, Siglec-7-mediated attenuation of NK and DC cell functions has been reported as an example of escape mechanisms of cancer cells from immune surveillance (4). Siglec-9 was isolated as a highly homologous gene to Siglec-7 (5). It is expressed in monocytes and granulocytes. Although inhibitory functions of Siglec-9 in immune cells via ITIM motifs have been reported in some experimental systems (6), outcome of the interaction between Siglecs and their sialylated ligands in the side of cells expressing sialyl-compounds has scarcely been studied to date.

During the analysis of effects of interaction between Siglec-9 and its counter ligands on cancer cells, we found marked degradation of focal adhesion kinase (FAK) in cancer cells, and also cell detachment from plates, suggesting apoptosis (7). Consequently, we have obtained interesting findings, suggesting novel implication of Siglec-9-mediated signaling in the regulation of adhesion dynamics of cancer cells.

EXPERIMENTAL PROCEDURES

Antibodies—Anti-human Siglec-9 (goat pAb IgG) was purchased from R&D system. Anti-FAK C-terminus antibody (rabbit pAb IgG) was purchased from Santa Cruz Biotechnology Inc. (Santa Cruz, CA), and anti-FAK N-terminus antibody (mouse mAb IgG1) was from BD. Anti-β-actin (mouse mAb IgG1) was purchased from Sigma-Aldrich. Anti-paxillin (mouse mAb IgG1), was from BD Transduction Laboratories. Anti-p130Cas (rabbit IgG, C-20), anti-FAK (rabbit IgG, C-20), anti-phospho FAK Tyr576-R (rabbit pAb) , FAK Tyr577-R (rabbit pAb), FAK Tyr861-R (rabbit pAb), FAK Tyr925-R (rabbit pAb) were from Santa Cruz Biotechnology. Anti--phospho-Akt Thr308 (rabbit mAb IgG), anti-phospho-Akt Ser473 (rabbit mAb IgG), anti-Akt (rabbit mAb IgG), anti-phospho-p130Cas Tyr165 (rabbit pAb), and anti-phospho-paxillin (Tyr118) (rabbit pAb) were from Cell Signaling Technology, Inc. (Beverly, MA). Anti-rabbit IgG conjugated with HRP, anti-mouse IgG conjugated with HRP was purchased from Cell Signaling Technology. Rabbit anti-goat-Alexa Fluor 488 was purchased from Invitrogen. Anti-SHP-1 (rabbit pAb IgG) was purchased from Millipore (Darmstadt, Germany).

Flow cytometry—Cell surface expression of Siglec-9Fc-binding ligands was analyzed by FACS Caliver^{TM} (Becton Dickinson, Franklin Lakes, NJ). Cells were incubated

with Siglec-9Fc (5 μg/100 μl in PBS) for 45 min on ice and then stained with FITC-conjugated anti-human IgG secondary antibody (Sigma) for 30 min on ice. Control cells for flow cytometry were prepared using the secondary antibody alone. For quantification of positive cells, CELLQuest™ program was used.

Neuraminidase treatment—To analyze whether sialic acids are essential for Siglec-9Fc binding, $1x10^6$ cells were applied in FACS tube, incubated with neuramidase (200 mU/ml) from *Vibrio cholera* (Roche Applied Science) for 1 h at 37 °C. Then, Siglec-9 binding was examined by flow cytometry as described below.

Flow cytometry and cell sorting—$U937^{siglec\text{-}9\text{-}high}$ cells and $U937^{mock}$ cells were suspended in cold PBS containing 2% FCS ($2x10^7$ cells/ml). To block non-specific binding, U937 cells were incubated with Fc (5 μg /100 μl PBS) for 15 min in dark on ice, then cells were labeled with goat anti-human Siglec-9 antibody (R&D) (10 μg) for 30 min on ice, then were washed 3 times with 2% FCS-containing PBS. Ten μg rabbit anti-goat IgG conjugated with Alexa488 was then added and incubated for 30 min. Cells were analyzed using FACSAria II™ (BD Bioscience, San Jose, CA). Normal goat IgG was used as a negative control. $U937^{siglec\text{-}9\text{-}high}$ cells were sorted from U937 transfected with pcDNA3.1-Siglec-9, $U937^{siglec\text{-}9\text{-}low}$ cells were sorted from $U937^{mock}$ cells. They were used for co-culture experiments as a positive or a negative group.

Productions of Siglec-9-Fc fusion proteins—pEE14-Siglec9-3C-Fc plasmid was generated by P.R. Crocker (8). pcDNA 3.1-Fc plasmid was designed in our laboratory. Siglec-9Fc and Fc secreted from HEK293T cells were prepared by DEAE-dextran transfection, and fusion proteins were affinity purified by Protein A Sepharose (Amersham Biosciences , Little Chalfont, UK). Protein concentration was measured by BCA Protein Assay Kit™ (Thermo).

Cell lines and culture—A human astrocytoma cell line AS (9) was maintained in RPMI1640 containing 10% fetal calf serum (FCS) at 37 °C in 5% CO_2 incubator. Siglec-9-over–expressing human histiocytic lymphoma (monocyte) $U937^{siglec\text{-}9\text{-}high}$ and $U937^{mock}$ cell lines were generated as described (10), both of which were maintained in RPMI1640 containing 10% FCS and G418 (450 μg/ml).

Real time cell electronic sensing (RT-CES) test—Cell adhesion and growth was dynamically monitored using the RT-CES system (SP v5.3) (ACEA Bioscience, CA). Cell index (CI) is a parameter used to represent cell adhesion status based on the electrical impedance in gold electrodes at the bottom of plates. CI was collected every 15 min. One $x10^4$ AS cells in 100 μl of RPMI1640 containing 10% FCS (regular medium) were seeded into the wells of 16-well e-plates (ACEA Bioscience), and cultured for 24 h. Then, $U937^{siglec\text{-}9\text{-}high}$ cells (10,000, 25,000 and 50,000) in 100 μl of the regular medium were added. Cells were co-cultured for 52 h or more in 200 μl volume at 37 °C in 5% CO_2 incubator. One $\times10^5$ of living or fixed $U937^{siglec\text{-}9\text{-}high}$ were added in the inhibitor experiments. For the fixation, U937 cells were washed with plain medium, and fixed with ethanol: acetic acid (95:5) for 20 min at 4 °C. They were washed 4 times with plain medium, then used for co-culture with AS. $U937^{siglec\text{-}9\text{-}low}$ cells were used as a negative control. For the stimulation with Siglec-9Fc or Fc proteins, $1x10^4$ AS cells in 200 μl of the regular medium were seeded in the wells of 16-well

e-plates. CI was monitored for 24 h, then 15 μg of Siglec-9Fc or Fc proteins were applied into e-plates, and CI was continuously monitored. All samples are duplicated and averages of results were used for statistical analysis. To examine whether degradation of FAK was caused by calpain, cells were pre-incubated with 25 μM of MDL-28170 (Calpain inhibitor III, Bachem AG, Bubendorf, Switzerland).

Co-culture experiments—AS cells were harvested using 2 mM EDTA/PBS, and seeded into 6-well plates at $1x10^5$/well, and maintained in the regular medium for 24 h at 37 °C. When growing cells covered about 70~75% area of the wells, medium was exchanged with plain RPMI1640 for deprivation of FCS. $U937^{siglec\text{-}9\text{-}high}$ and $U937^{siglec\text{-}9\text{-}low}$ cells were incubated in FCS-free RPMI1640 for 4 h, then $1x10^6$ of $U937^{siglec\text{-}9\text{-}high}$ and $U937^{siglec\text{-}9\text{-}low}$ cells were added and co-cultured with AS cells. U937 cells were carefully removed without disturbing AS cells by washing twice with plain RPMI1640. Cells were harvested at 5, 15 and 30 min after co-culture, then lysed with 1x lysis buffer (Cell Signaling) containing protease inhibitor cocktail I (Calbiochem) and 1 mM PMSF (WAKO, Osaka, Japan). Protein concentration was measured by BCA Protein Assay Kit™ (Thermo).

Immunoblotting of SHP-1—To examine whether Siglec-9 recruits protein tyrosine phosphatase 1 (SHP-1) in U937 cells after co-culture with AS, $U937^{siglec\text{-}9\text{-}high}$ and $U937^{siglec\text{-}9\text{-}low}$ co-cultured with AS for 15 and 30 min were used as sources of cell lysates. U937 cell lysates (300 μg) were precipitated with 2 μg of anti-human Siglec-9 antibody and Protein G Sepharose™ (Amersham Biosciences), and the precipitates were served for immunoblotting with anti-SHP-1 antibody.

Wound healing assay—Migration activity of AS cells co-cultured with $U937^{siglec\text{-}9\text{-}high}$ or $U937^{siglec\text{-}9\text{-}low}$ was assessed by scratching assay. AS cells were plated in 6-well plates ($1 x10^5$/well) and cultured for 48 h in 10% FCS-containing RPMI1640 medium. When the cells reached 90% confluency, a scratch was generated using a 200 μl sterile tip. To remove cell debris, each well was rinsed twice with plain RPMI1640 medium before co-culture. Then, the cells were overlaid with $U937^{siglec\text{-}9\text{-}high}$ or $U937^{Siglec\text{-}9\text{-}low}$ cells ($1x10^6$/well), and cultured continuously for 24 h. The wound area images were photographed by a CCD camera (Olympus DP11, Olympus IX70) after carefully removing U937 cells by washing twice with plain RPMI1640 at time 0, 12 and 24 h after the scratching. Wound healing spaces were measured using ImageJ v1.47d (NIH, http://rsb.info.nih. gov/ij/). The wound-closure rates were obtained at 3 independent sites in the individual groups.

Cell migration assay with Boyden chamber—Matrigel-coated chambers (BD Biosciences) were rehydrated according to the manufacturer's instruction. AS cells were detached by 2 mM EDTA/PBS, and were applied into rehydrated upper chamber at $1×10^5$/ml in RPMI1640 (10% FCS). Three ml of RPMI1640 (10% FCS) was applied into the lower chamber. At 15 min after plating cells, $U937^{siglec\text{-}9\text{-}high}$ or $U937^{siglec\text{-}9\text{-}low}$ cells were overlaid at $1x10^6$/ml in RPMI1640 (10% FCS). After co-culture for 24 h at 37°C, upper chamber was fixed in 70% ethanol for 5 min, then upper surface of the chamber was wiped with cotton swabs without disturbing lower surfaces. The lower surface of the chamber was stained by Giemsa solution, and 10 random fields of the stained membranes were photographed by CCD camera

(Olympus DP11, Olympus IX70). Then, cell number was counted by a cell counter plugin of ImageJ v1.47d (*NIH, http://rsb.info.nih.gov/ij/*) software.

Immunoblotting—To examine signaling pathways in AS and other cell lines, cell lysates (15 μg) were separated by SDS-PAGE using 8% gels, and separated proteins were transferred onto a PVDF membrane (Millipore). Blots were blocked with 5% BSA in TBS containing 0.05% Tween-20 (TBST) for more than 6 h at 4°C. The membrane was first probed with primary antibodies. After being washed, the blots were then incubated with goat anti-rabbit IgGs or horse anti-mouse IgGs conjugated with HRP (1:2000). After washing, bound conjugates were visualized with an ECL™ detection system (PerkinElmer, Waltham, MA). Band intensities were analyzed with Image J (NIH, http://rsbweb.nih.gov/ij/) and standardized with β-actin.

RESULTS

To determine the expression of Siglec-9 ligand-carrier molecules expressed on cancer cells, we performed flow cytometry using 75 human cancer cell lines. Simultaneously, Siglec-9 ligand-carrier molecules were isolated and identified using Siglec-9Fc (8) and mass spectrometry.

Majority of all tested cell lines showed fairly high expression levels of Siglec-9 ligands on the cell surface as shown in Supplemental Table S1. According to the score of mean fluorescence intensity, we used a human astrocytoma cell line AS in following experiments as one of the Siglec-9 ligand-high-expressing cells (Fig. 1A). Identified proteins as Siglec-9 ligand-carrier molecules were summarized in Supplemental Table S2. Results of further analysis will be reported elsewhere.

Sialic acid dependent binding of Siglec-9 was confirmed using neuraminidase as shown in Fig. 1B. To examine the effects of the interaction between immune cells and cancer cells via Siglec-9 on the signaling pathway in both sides of cells, co-culture experiments with U937 and AS were performed. Stable transfectant cell lines, $U937^{siglec\text{-}9\text{-}high}$ and $U937^{siglec\text{-}9\text{-}low}$ were established as shown in Fig. 1C. These two transfectant lines were apparently similar suspension cells with no attachment to culture dishes. Morphological features of these cells were shown in Fig. 1D. AS cells are adherent cells and U937 cells are suspension cells (leukemia), and their sizes are quite different, which allowed us to visually distinguish and experimentally separate them each other very easily.

Co-culture assay was performed by real-time cell electronic sensing (RT-CES) system as described in Experimental Procedures. This system could assess the effect of interaction between AS cells and Siglec-9-expressing U937 cells on AS cells by measuring CI. Intensities of cell adhesion and spreading can be monitored in a real-time manner. Three kind of stimulants were used, i.e. living U937 cells, fixed ones and soluble Siglec-9Fc or Fc proteins.

CI of AS decreased after co-culture with living $U937^{siglec\text{-}9\text{-}high}$ cells at 63 h ($5x10^4$) and 71 h ($2.5x10^4$) of culture. No decrease in CI was found in AS co-cultured with $U937^{siglec\text{-}9\text{-}low}$ cells (Fig. 2A). When AS was co-cultured with fixed $U937^{siglec\text{-}9\text{-}high}$, detachment of AS was detected immediately after addition of U937 cells. To examine the fates of detached cells, FCS concentration was increased up to 10%, resulting in the re-attachment and re-growth of AS cells as shown in RT-CES (Fig 2B). These features

were also observed in a morphological approach (Fig. S1A). Immediate decrease of cell adhesion was detected when AS cells were treated by soluble Siglec-9Fc (150 μg/ml) in the regular medium, while it was gradually restored in CI (Fig. 2C).

Considering the possibility of the cell detachment represented cell deterioration due to toxic effects of Siglec-9 binding, immunoblotting for activated Caspase-3 and FACS analysis of Annexin V/propidium iodide (PI) was performed (Fig. S1B and C). Neither activated Caspase-3 nor apoptosis induction was found in AS cells after co-culture with U937$^{siglec\text{-}9\text{-}high}$ cells for 16 h in FCS-free condition. Higher levels of cell death were found rather in AS co-cultured with U937$^{siglec\text{-}9\text{-}low}$ (7% vs. 1.76%) (Fig. S1C). Furthermore, SHP-1 was recruited at Siglec-9 in U937$^{siglec\text{-}9\text{-}high}$ cells at 15 and 30 min after co-culture with AS, while no recruitment of SHP-1 was detected in U937$^{siglec\text{-}9\text{-}low}$ cells (Fig. 3). This result suggested that Siglec-9 triggered inhibitory signals in U937 via the interaction with its ligands on AS as expected. No significant differences in cell growth activity were found during co-culture for 7 days in AS (Fig. S1D).

Cell motility and invasion of AS was examined by wound healing assay and cell migration assay, respectively, when they were co-cultured with U937$^{siglec\text{-}9\text{-}high}$ or U937$^{siglec\text{-}9low}$ cells. In wound healing assay, AS cells co-cultured with U937$^{siglec\text{-}9\text{-}high}$ showed significantly higher motility than the negative control and untreated cells (Fig. 4A, B). In Boyden chamber assay, AS cells co-cultured with U937$^{siglec\text{-}9\text{-}high}$ also showed higher cell invasion than those co-cultured with U937$^{siglec\text{-}9\text{-}low}$ (Fig. 4C, D).

To investigate what occurred in AS cells co-cultured with U937 with high or low levels of Siglec-9, we examined activation of representative proteins. To our surprise, total FAK bands dramatically decreased in AS co-cultured with U937$^{siglec\text{-}9\text{-}high}$. Accordingly, all phosphorylation site-specific FAK bands showed definite reduction in the band intensities (Fig. 5A, 5B). Minimal changes in FAK and/or phosphorylated FAK were found in AS co-cultured with U937$^{siglec\text{-}9\text{-}low}$.

Immunoblotting data of signaling proteins such as Akt, paxillin and Crk-associated substrate protein (p130Cas) showed that they also underwent reduction in the band intensities (Fig. 5C-F). In particular, total Akt band showed marked degradation, while phosphorylation bands at T308 and S473 did not reduce (Fig. 5C, D). Bands of p-Akt T308 rather increased in U937$^{siglec\text{-}9\text{-}high}$-treated cells at 15 min. Phosphorylated bands of paxillin and p130Cas also showed no changes (Fig. 5E, F). No significant differences were found during co-culture with U937$^{siglec\text{-}9\text{-}low}$. By the treatment of AS cells with soluble Siglec-9Fc, similar degradation of FAK, Akt, p130Cas and paxillin was also found, while Fc protein alone showed no effects (Fig. 6A-D). When complex of Siglec-9Fc with anti-human IgG $F(ab')_2$ was used, stronger degradation of FAK was found than in A (Fig. 6E). No significant differences in band intensities of total ERKs and Src, and their phosphorylation forms were found between cells co-cultured with U937$^{siglec\text{-}9\text{-}high}$ and those with U937$^{siglec\text{-}9\text{-}low}$ (Fig. S2A, B).

To clarify spatio-temporal dynamics of the protein degradation and its implication in cell behaviors, time course of the degradation and intracellular localization of FAK and p-Akt were analyzed by immunoblotting and immunocytochemistry, respectively. As shown in Fig. 7, FAK levels were restored at 12-24 h after addition of FCS, while p-Akt T308 levels increased in earlier stage (~60

min), probably reflecting increased cell motility in AS cells treated with U937$^{siglec-9-high}$.

Immunocytochemistry revealed that FAK staining was markedly reduced in U937 $^{siglec-9-high}$-treated AS and remaining FAK was found only one side of cytoplasm compared with AS cells treated with U937$^{siglec-9-low}$, in which FAK was distributed highly and broadly in the cytoplasm (Fig. 8 A). Furthermore, simultaneous staining of FAK and p-Akt T308 revealed that these two molecules were localized at the same side of cells, probably front region of cells (Fig. 8B). Details were shown in SI (Fig. S4).

Degradation of FAK through Siglec-9 was examined in another cell lines, i.e. an ovarian cancer cell line (HEY) and a glioma cell line (U251). They showed similar FAK degradation during co-culture with U937$^{siglec-9-high}$ (Fig. 9A) that indicated universality of the results with AS cells. Results of RT-CES also showed similar reduction of CI and subsequent restoration after FCS treatment as observed in AS (Fig. 9B).

Sialic acid dependency of these protein degradation was examined by pre-treatment of AS cells with neuraminidase before co-culture, resulting in the reduced degradation as expected (Fig. S3).

To clarify whether the dynamic changes of bands in FAK, Akt and so on during the co-culture of AS cells with U937$^{siglec-9-high}$ cells were protein degradation due to proteolytic enzymes, blocking of calpain was performed, since calpain seemed to be the most likely protease responsible for the cleavage of FAK (11). In RT-CES, AS cells treated with U937$^{siglec-9-high}$ and a calpain inhibitor MDL-28170 caused apparently less reduction of CI than those with U937$^{siglec-9-high}$ alone (Fig. 10A). This was particularly clear when AS was treated with fixed U937$^{siglec-9-high}$ and MDL-28170. These cells showed almost same pattern (no reduction of CI) as untreated cells (Fig. 10B), while AS cells treated with fixed U937$^{siglec-9-high}$ alone showed definite CI reduction. This was also the case when AS was treated by Siglec-9Fc (Fig. 10C).

By the treatment of AS cells with 25 μM of MDL28170 before co-culture with U937$^{siglec-9-high}$, degradation of FAK was completely suppressed (Fig. 11A, B). This was also the case for Akt, p130Cas and paxillin (Fig. 11C, D), strongly suggesting that calpain was responsible for the degradation of these molecules.

All these results were summarized in Fig. 12.

DISCUSSION

Majority of past studies on Siglec-mediated signaling have been done about ITIM-associated inhibitory signals in immune cells. There have been no reports on the signaling in cancer cells that express counter receptors with sugar chains recognized by Siglecs. In this study, we demonstrated, for the first time, that Siglec-9 triggered a signal, leading to degradation of FAK, Akt and related molecules in cancer cells. Most novel point in this study is that cancer cells receive not death signals, but a sort of activation signals via interaction between Siglec-9 on immune cells and its counter receptors on cancer cells. Furthermore, it was clearly shown that all observed differences in Fig. 2~Fig. 5 were due to the interaction between Siglec-9 and sialylglycoconjugates/carrier proteins, since the presence/absence of Siglec-9 on U937 was sole difference in our system, and the removal of sialic acids clearly cancelled Siglec-9 binding and FAK degradation.

FAK is a tyrosine kinase playing multi-functions in the cell signaling for cell adhesion (12), proliferation (13), migration (14) and cancer metastasis (12, 13). FAK is present mainly at the focal adhesion and plays essential roles by interacting with various signaling molecules such as p130Cas, paxillin and Src-family kinases (15). We have investigated roles of FAK in the enhanced malignant properties such as cell proliferation (16) and cell adhesion to extracellular matrix (ECM) (17) in malignant melanomas expressing ganglioside GD3. Apoptosis induction of small cell lung cancer cells by anti-ganglioside GD2 monoclonal antibodies via dephosphorylation of FAK was also reported by us (7). In addition to enhanced adhesion to ECM, increased migration and cell motility are also a hallmark of cancer cells (18). FAK has been considered to regulate cell migration by orchestrating signals between growth factor receptors and integrins (19). Although FAK is important in the cell adhesion in association with integrins, it is also essential for the regulation of focal adhesion disassembly (20). Degradation of FAK might be important for the promotion of cell migration by regulation of adhesion dynamics (11).

In our results, FAK underwent rapid degradation in cancer cells after co-culture with Siglec-9-expressing cells. Representative tyrosine-phosphorylated forms of FAK also degraded along with total FAK. On the other hand, cell migration and invasion activities increased after co-culture. These paradoxical results might indicate the differences in the roles of FAK depending on the spatial and temporal dynamics of cell adhesion and migration as shown in Fig. 12. Other signaling molecules than FAK showed sustained levels of individual phosphorylated forms during co-culture, suggesting partially overlapping activation of those molecules with FAK degradation. Among molecules that showed sustained activated levels, we focused on p-Akt T308 because of its increased phosphorylation in the early phase of co-culture, and could show its localization in the front side of AS cells as well as remaining FAK. These results should explain, at least partly, mechanisms for the increased migration of AS cells undergoing FAK degradation as shown in Fig. 12. Increased activation of Akt T308 as shown in Fig. 5C and D might be also involved in the resistance to apoptosis in AS (21). Details in the spatio-temporal regulation of FAK molecules as well as its related molecules in the cell migration remain to be investigated.

Results obtained in this study suggested that proteolytic enzymes should be activated and exert for the transient degradation of a wide range of signaling molecules. Possible protease responsible for the degradation of FAK etc should be calpain (11, 22) as revealed by its inhibitor. Results of experiments for mobility and apoptosis also support the concept that the protein degradation observed in co-culture might be beneficial for cancer cell migration and survival in addition to the simultaneously induced inhibitory signals in immune cells (U937 in this study), leading to the escape from immunosurveillance. Thus, sialylated complex carbohydrates expressed on the cell surface of cancer cells might play very important roles in the two-directions, i.e. transduction of inhibitory signals in immune cells via Siglec-9 and of activation signals to lead activation of calpain and subsequent increases in cell motility and survival of cancer cells.

Significances of the degradation of Akt, paxillin and p130Cas are not clear at this

moment. However, phosphorylated Akts, paxillin and p130Cas did not reduce or sometimes increased during the co-culture, suggesting that they undergo differential regulation and exert distinct roles depending on the phosphorylation status.

The facts that not only Siglec-9-expressing living cells, but also fixed Siglec-9-expressing cells and even soluble Siglec-9 proteins could induce similar cell responses such as cell detachment from plates and increased cell movement strongly suggested that cell surface Siglec-9 actually triggers counter signals in cancer cells via Siglec-9-recognizing sugar chains. Since binding specificity of Siglec-9 is broad (2, 4), multiple molecules may be recognized by Siglec-9 as shown in Table S2. Although it is not easy to identify crucial molecules as functional counter receptors for Siglec-9 in cancer cells, identification of such counter receptors carrying sialylglycoconjugates should allow us to focus target molecules for the cancer therapeutics. These trials are now on-going in our group.

Acknowledgments—*We thank P.R. Crocker at Dundee University for kindly providing an expression vector for Siglec-9Fc. We also thank T. Mizuno and Y. Nakayasu for technical assistance.*

This study was supported by a Grant-in-Aid for Scientific Research (21390076, 24390078), and partly by a Grant-in-Aid for Scientific Research (23590371), by a Grant-in-Aid for Scientific Research on Innovative Areas (No. 23110008) from MEXT, and Grants of Toyoaki Shogaku-kai Foundation and Kobayashi Foundation.
There is no conflict of interest.

Appendix Supplemental data associated with this article can be found in the online version.

REFERENCES

1. Varki, N. M., and Varki, A. (2007) Diversity in cell surface sialic acid presentations: implications for biology and disease. *Lab Invest* **87**, 851-857
2. Lehmann, F., Tiralongo, E., and Tiralongo, J. (2006) Sialic acid-specific lectins: occurrence, specificity and function. *Cell Mol Life Sci* **63**, 1331-1354
3. Crocker, P. R., Paulson, J. C., and Varki, A. (2007) Siglecs and their roles in the immune system. *Nat Rev Immunol* **7**, 255-266
4. Pillai, S., Netravali, I. A., Cariappa, A., and Mattoo, H. (2012) Siglecs and immune regulation. *Annu Rev Immunol* **30**, 357-392
5. Angata, T., and Varki, A. (2000) Cloning, characterization, and phylogenetic analysis of siglec-9, a new member of the CD33-related group of siglecs. Evidence for co-evolution with sialic acid synthesis pathways. *J Biol Chem* **275**, 22127-22135
6. Ohta, M., Ishida, A., Toda, M., Akita, K., Inoue, M., Yamashita, K., Watanabe, M., Murata, T., Usui, T., and Nakada, H. (2010) Immunomodulation of monocyte-derived dendritic

cells through ligation of tumor-produced mucins to Siglec-9. *Biochem Biophys Res Commun* **402**, 663-669

7. Aixinjueluo, W., Furukawa, K., Zhang, Q., Hamamura, K., Tokuda, N., Yoshida, S., and Ueda, R. (2005) Mechanisms for the apoptosis of small cell lung cancer cells induced by anti-GD2 monoclonal antibodies: roles of anoikis. *J Biol Chem* **280**, 29828-29836
8. Zhang, J. Q., Nicoll, G., Jones, C., and Crocker, P. R. (2000) Siglec-9, a novel sialic acid binding member of the immunoglobulin superfamily expressed broadly on human blood leukocytes. *J Biol Chem* **275**, 22121-22126
9. Watanabe, T., Pukel, C. S., Takeyama, H., Lloyd, K. O., Shiku, H., Li, L. T., Travassos, L. R., Oettgen, H. F., and Old, L. J. (1982) Human melanoma antigen AH is an autoantigenic ganglioside related to GD2. *J. Exp. Med.* **156**, 1884-1889
10. Mitsuki, M., Nara, K., Yamaji, T., Enomoto, A., Kanno, M., Yamaguchi, Y., Yamada, A., Waguri, S., and Hashimoto, Y. (2010) Siglec-7 mediates nonapoptotic cell death independently of its immunoreceptor tyrosine-based inhibitory motifs in monocytic cell line U937. *Glycobiology* **20**, 395-402
11. Chan, K. T., Bennin, D. A., and Huttenlocher, A. (2010) Regulation of adhesion dynamics by calpain-mediated proteolysis of focal adhesion kinase (FAK). *J Biol Chem* **285**, 11418-11426
12. Golubovskaya, V. M. (2010) Focal adhesion kinase as a cancer therapy target. *Anticancer Agents Med Chem* **10**, 735-741
13. Hall, J. E., Fu, W., and Schaller, M. D. (2011) Focal adhesion kinase: exploring Fak structure to gain insight into function. *Int Rev Cell Mol Biol* **288**, 185-225
14. Zhao, X., and Guan, J. L. (2011) Focal adhesion kinase and its signaling pathways in cell migration and angiogenesis. *Adv Drug Deliv Rev* **63**, 610-615
15. Schaller, M. D. (2010) Cellular functions of FAK kinases: insight into molecular mechanisms and novel functions. *J Cell Sci* **123**, 1007-1013
16. Hamamura, K., Tsuji, M., Ohkawa, Y., Nakashima, H., Miyazaki, S., Urano, T., Yamamoto, N., Ueda, M., and Furukawa, K. (2008) Focal adhesion kinase as well as p130Cas and paxillin is crucially involved in the enhanced malignant properties under expression of ganglioside GD3 in melanoma cells. *Biochim Biophys Acta* **1780**, 513-519
17. Ohkawa, Y., Miyazaki, S., Hamamura, K., Kambe, M., Miyata, M., Tajima, O., Ohmi, Y., Yamauchi, Y., and Furukawa, K. (2010) Ganglioside GD3 enhances adhesion signals and augments malignant properties of melanoma cells by recruiting integrins to glycolipid-enriched microdomains. *J Biol Chem* **285**, 27213-27223
18. Friedl, P., and Gilmour, D. (2009) Collective cell migration in morphogenesis, regeneration and cancer. *Nat Rev Mol Cell Biol* **10**, 445-457
19. Sieg, D. J., Hauck, C. R., and Schlaepfer, D. D. (1999) Required role of focal adhesion kinase (FAK) for integrin-stimulated cell migration. *J Cell Sci* **112 (Pt 16)**, 2677-2691
20. Webb, D.J., Donals, K., Whitmore, L.A., Thomas, S.M., Turner, C.E., Parsons, J.T., Horwitz, A.F. (2004) FAK–Src signalling through paxillin, ERK and MLCK regulates adhesion disassembly. *Nat Cell Biol* **6,** 154-161
21. Li, B., Desai, S.A., MacCorkle-Chosnek, R.A., Fan, L., Spencer, D.M. (2002) A novel conditional Akt 'survival switch' reversibly protects cells from apoptosis. *Gene Ther* **9,**

233-244
22. Frame, M.C., Fincham, V.J., Carragher, N.O., Wyke, J.A. (2002) v-Src's hold over actin and cell adhesions. *Nat Rev Mol Cell Biol* **3,** 233-245

Figure legends

Figure 1. Cancer cells expressing ligands for Siglec-9 and effector cells expressing Siglec-9 on the cell surface. A, Seventy five human cell lines were screened for binding of Siglec-9Fc by flow cytometry. Representative examples (AS, astrocytoma; TUHR10-TKB, renal cell cancer) were shown. B, Characterization of glycans recognized by Siglec-9 using neuraminidase. Siglec-9 binding reduced after treatment with neuramidase (200 mU/ml) in 3 cell lines. Definite reduction in the binding intensities of Siglec-9Fc was observed in AS (93.4%; MFI: 345.1 vs. 22.7), SK-MEL-28 (melanoma) (95.5%; MFI: 284.3 vs. 12.7) and SK-LC-10 (lung cancer) (98.9%; MFI: 332.7 vs. 3.6). C, U937$^{\text{siglec-9-high}}$ and U937$^{\text{siglec-9-low}}$ clones used in co-culture system. Full length of Siglec-9 cDNA was transfected into U937, and sorted by labeling with anti-human Siglec-9 antibody using FACSAria II^{TM}, resulting in the establishment of U937$^{\text{siglec-9-high}}$ and U937$^{\text{siglec-9-low}}$. D, Morphological features of these cells were shown (x200).

Figure 2. RT-CES of AS co-cultured with U937$^{\text{siglec-9-high}}$ and U937$^{\text{siglec-9-low}}$, or treated with soluble Siglec-9Fc. A, Cell index (CI) of AS (1×10^4 cells) co-cultured with U937 cells (10,000, 25,000 and 50,000 cells) was examined. B, CI of AS co-cultured with U937 cells fixed in ethanol: acetic acid was examined. One x10^4 AS were maintained in RPMI1640 containing 10% FCS, then U937 cells (1×10^5) were added (final FCS: 3.5%). When FCS was added up to 10%, U937$^{\text{siglec-9-high}}$-treated AS re-attached and re-grew. C, CI of AS treated with Siglec-9Fc or Fc proteins (150 μg/ml). All samples were analyzed by duplicated, and average values of similar results (less than 5% differences) were shown. These experiments were repeated at least 3 times with similar results.

Figure 3. Immunoblotting of SHP-1. Recruitment of SHP-1 in U937 cells co-cultured with AS was examined at 15 and 30 min. U937$^{\text{siglec-9-high}}$ and U937$^{\text{siglec-9-low}}$ co-cultured with AS for 15 and 30 min were lyzed, then 300 μg of the lysates was precipitated with 2 μg of anti-human Siglec-9 antibody (R&D system) and protein G Sepharose (GE Healthcare). The precipitates were immunoblotted by anti-SHP-1 antibody. No recruitment of SHP-1 was found in U937$^{\text{siglec-9-low}}$ cells, while definite bands were detected in U937$^{\text{siglec-9-high}}$ cells. This experiment was repeated at least 3 times with similar results.

Figure 4. Effects of co-culture on AS properties. A, Wound healing scratching assay was performed as described in Experimental Procedures, and representative results of AS cell migration were shown (x100) at time 0, 12, 24 h co-culture. B, Results in A was presented as covered areas (%). Untreated AS (control) covered 37.7% (12 h) and 57% (24 h). AS co-cultured with U937$^{\text{siglec-9-low}}$ showed similar results. AS co-cultured with U937$^{\text{siglec-9-high}}$ showed significantly higher motility than these two ($p<0.01$). C, Invasion of AS cells during co-culture. AS cell invasion activity in Matrigel-coated Boyden chamber was measured. Representative images of stained cells were shown (x200). Invasion of AS increased after co-culture with U937$^{\text{siglec-9-high}}$ for 24 h compared with those co-cultured with U937$^{\text{siglec-9-low}}$ ($N=10$, $p<0.01$).

Figure 5. Degradation of FAK, Akt, p130Cas and paxillin in AS during co-culture with U937$^{siglec\text{-}9\text{-}high}$. AS cells were co-cultured with U937 cells for 5, 15 and 30 min, and total protein samples were harvested. Fifteen μg proteins were tested in immunoblotting. A, Results of immunoblotting for total FAK and phosphorylated FAK at Y576, Y577, Y861 and Y925 in AS cells during co-culture with U937 cells. β-actin was used for loading control. B, Results of the densitometric analysis of total FAK and phosphorylated FAKs. Results are shown as expression and/or phosphorylation levels of FAK after normalization with band intensities of β-actin. C, Results of immunoblotting for total Akt and phosphorylated forms at T308 and S473 in AS cells treated as in A. D, Results of the densitometric analysis of total Akt and phosphorylated Akts. Results are shown as described in B. E, Results of immunoblotting for p130Cas and paxillin in AS cells treated as in A and C. F, Results of the densitometric analysis of total p130Cas and paxillin and phosphorylated forms as shown in B and D. These experiments were repeated at least 3 times with similar results.

Figure 6. Degradation of FAK and related molecules by addition of Siglec-9Fc. Five×10^4 AS cells were seeded in 6-well plates, and cultured in 10% FCS-containing RPMI1640 for 24 h. Then, medium was exchanged with FCS free medium, and cells were incubated for 12 h. Siglec-9Fc or Fc proteins (20 μg) was then added to the wells. After15 and 30 min incubation, AS cells were harvested for immunoblotting. Fifteen μg each of protein was applied to 8% SDS-PAGE. Then wet transferred onto PVDF membrane, and detected by anti-FAK (A), anti-Akt (B), anti-p130Cas (C) and anti-paxillin (D) antibodies as described in Fig. 5. E, Effects of Siglec-9Fc cross-linked by anti-human IgG Fc secondary antibody. To AS cells prepared as in A, preformed Siglec-9Fc and secondary antibody complex (5 or 20 μg each) was added. Anti-human IgG F(ab')$_2$ fragment (Sigma) was used by mixing in 200 μl PBS before incubation for 2 h at room temperature. Fc fusion protein in stead of Siglec-9Fc was used as a negative control. After 15 and 30 min incubation, AS cells were washed and harvested for immuno-blotting. Fifteen μg each of protein was applied to 8% SDS-PAGE, then detected by anti-FAK (N-term) antibody. *, non-specific band; deg, degradation products.

Figure 7. Restoration of FAK and Akt, and phosphorylation of Akt T308 in AS cells treated with 10% FCS after co-culture. Co-culture with U937$^{siglec\text{-}9\text{-}high}$ cells was performed as described in Fig. 5, then 10% FCS was added to culture medium after 30 min of co-culture after removal of U937 $^{siglec\text{-}9\text{-}high}$ cells (*left*) or in the presence of U937$^{siglec\text{-}9\text{-}high}$ cells (*right*), then incubated up to 24 h. At the individual time points, AS cells were harvested, then cell lysates were applied for immunoblotting for FAK (A), and Akt (total Akt (*lower*) and p-Akt (*upper*)) (B) as described in the legend for Fig. 5. *, non-specific band; deg, degradation products.

Figure 8. FAK degradation during co-culture shown by immunocytochemistry. Six×10^4 AS cells were seeded in glass-based dishes (Iwaki), and cultured for 1~2 days, then FCS was starved for 12 h. AS cells were co-cultured with 1× 10^6 U937 $^{Siglec\text{-}9\text{-}high}$ or U937 $^{Siglec\text{-}9\text{-}low}$ cells. After co-culture for 30 min, U937 cells were removed by washing with plain medium. Cells were fixed with 4% paraformaldehyde, then permeabilized with 0.1% Triton X-100/PBS (pH 7.2). After being blocked with 5% BSA/PBS for 1 h, cells were stained with anti-FAK antibody

at 1:400 dilution for 1 h at room temperature, then incubated with rabbit anti-mouse IgG Alexa-568 secondary antibody (red) (Invitrogen) at 1:400 dilution for 60 min in dark. Then cell nucleus was stained with Hoechst 33342 (1:10000 dilution) (light blue) for 15 min. Finally, cells were observed with FV10i^{TM} Laser Scanning Confocal Microscope (Olympus, Japan). Cell images were analyzed by FV10-ASW Viewer^{TM} (version 3.01). Low magnification images (*Upper*) and high magnification images (*Lower*) were shown. Scale bar, 25 μm. B, cells were stained with anti-FAK antibody as in A and anti-p-Akt T308 (rabbit IgG, Cell signaling, at 1:400 dilution) for 60 min at RT. Then, cells were stained with Alexa Fluor 555-goat anti-mouse IgG1 for FAK (Invitrogen)(1:400 dilution) and Alexa Fluor 488-goat anti-rabbit IgG (H+L) antibody (Invitrogen) for p-Akt T308. Cells were also stained with Hoechst 33342. Details for image analysis and individual images were shown in SI (Fig. S4). Co-staining pattern of FAK, p-Akt and nucleus in U937$^{siglec\text{-}9\text{-}high}$-treated AS was shown. Scale bar, 10 μm.

Figure 9. Degradation of FAK in HEY (ovarian cancer) and U251 (astrocytoma) during co-culture with U937$^{siglec\text{-}9\text{-}high}$. HEY and U251 cells were co-cultured with U937 cells as described above for AS cells. A, Results of immunoblotting for FAK. Anti-FAK (N-terminus) antibody was used (*upper*). Note that strong FAK degradation was observed during co-culture with U937$^{siglec\text{-}9\text{-}high}$ as observed in AS. Results of the densitometric analysis of FAK are shown after normalization with band intensities of β-actin as in Fig. 5 (*lower*). B, CI of U251 cells (*upper*) or HEY cells (*lower*) co-cultured with fixed U937 cells was examined. One x10^4 cells were maintained in RPMI1640 containing 10% FCS, then U937 cells (1×10^5) were added (final FCS: 3.5%). After 24 h, FCS was added up to 10% as indicated to examine the restoration of cell growth as in Fig. 2. These experiments were repeated at least 3 times with similar results.

Figure 10. Calpain is responsible for the detachment of AS cells co-cultured with U937. MDL28170 prevented cell detachment of AS during co-culture with U937$^{siglec\text{-}9\text{-}high}$. One x$10^4$ AS cells were cultured for 20 h in 100 μl of the regular medium with or without MDL28170 (25 μM), then were co-cultured with 1x10^5 of U937$^{siglec\text{-}9\text{-}high}$ (A), fixed U937$^{siglec\text{-}9\text{-}high}$ (B), or Siglec-9-Fc/Fc proteins (150 μg/ml)(C). Note that MDL28170 treatment prevented AS from the detachment. These experiments were repeated at least 3 times with similar results.

Figure 11. Complete protection of protein degradation with a calpain inhibitor, MDL28170. Effects of a calpain inhibitor on the protein degradation of FAK (A), Akt, p130Cas and paxillin (C) were examined. A, AS cells were treated with MDL28170 (25 μM), and co-cultured and immunoblotted as described. B, Band intensities in A were measured and presented after normalization with those of β-actin. C, Degradation of Akt, p130Cas and paxillin was also examined to analyze effects of MDL28170 on their degradation in AS during co-culture with U937$^{siglec\text{-}9\text{-}high}$. Immunoblotting was performed as described above. D, Results of the densitometric analysis of bands of Akt, p130Cas and paxillin shown in C were presented after normalization with those of β-actin.

Figure 12. A schema to show the results demonstrated in this paper.

Fig. 1

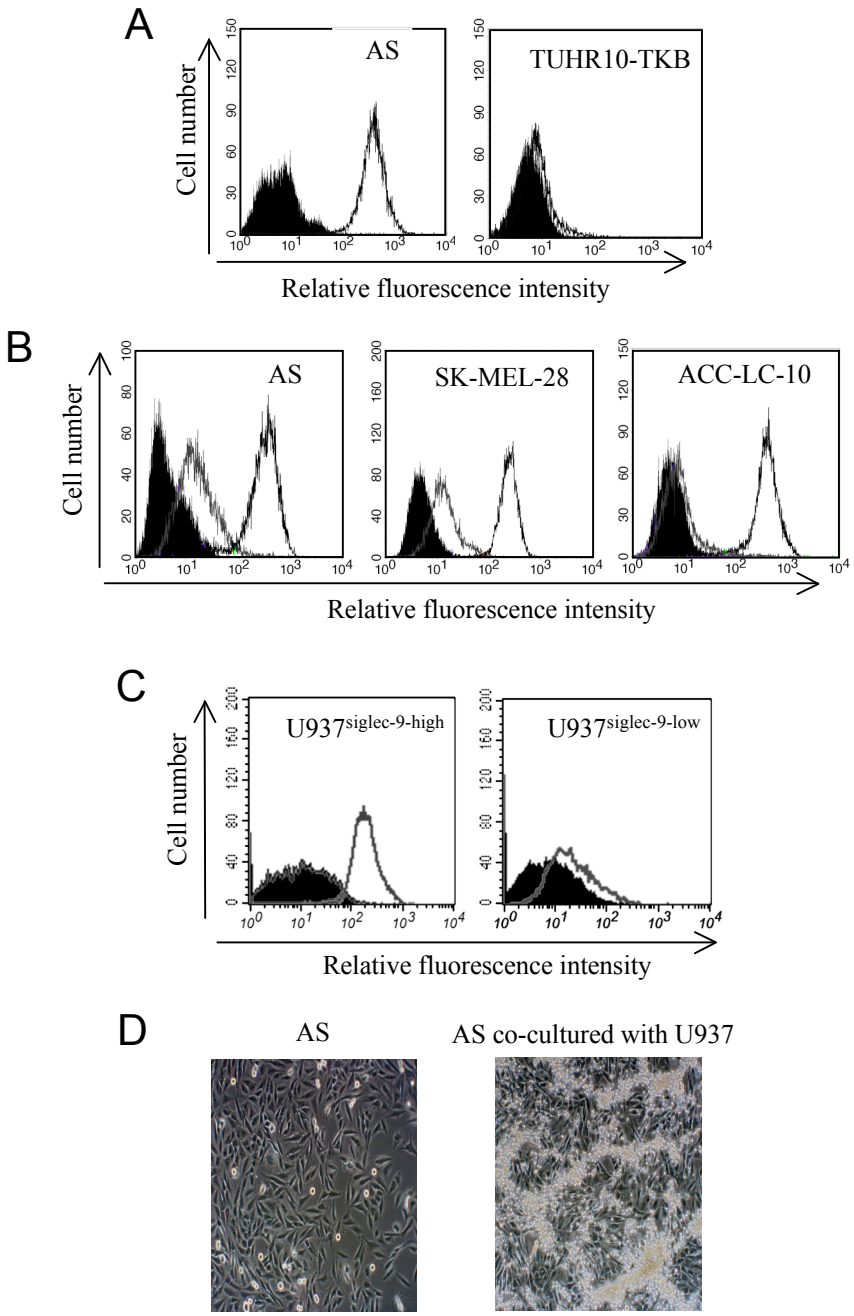
A
AS
TUHR10-TKB
Cell number
Relative fluorescence intensity
B
AS
SK-MEL-28
ACC-LC-10
Cell number
Relative fluorescence intensity
C
U937siglec-9-high
U937siglec-9-low
Cell number
Relative fluorescence intensity
D
AS
AS co-cultured with U937

Fig. 2

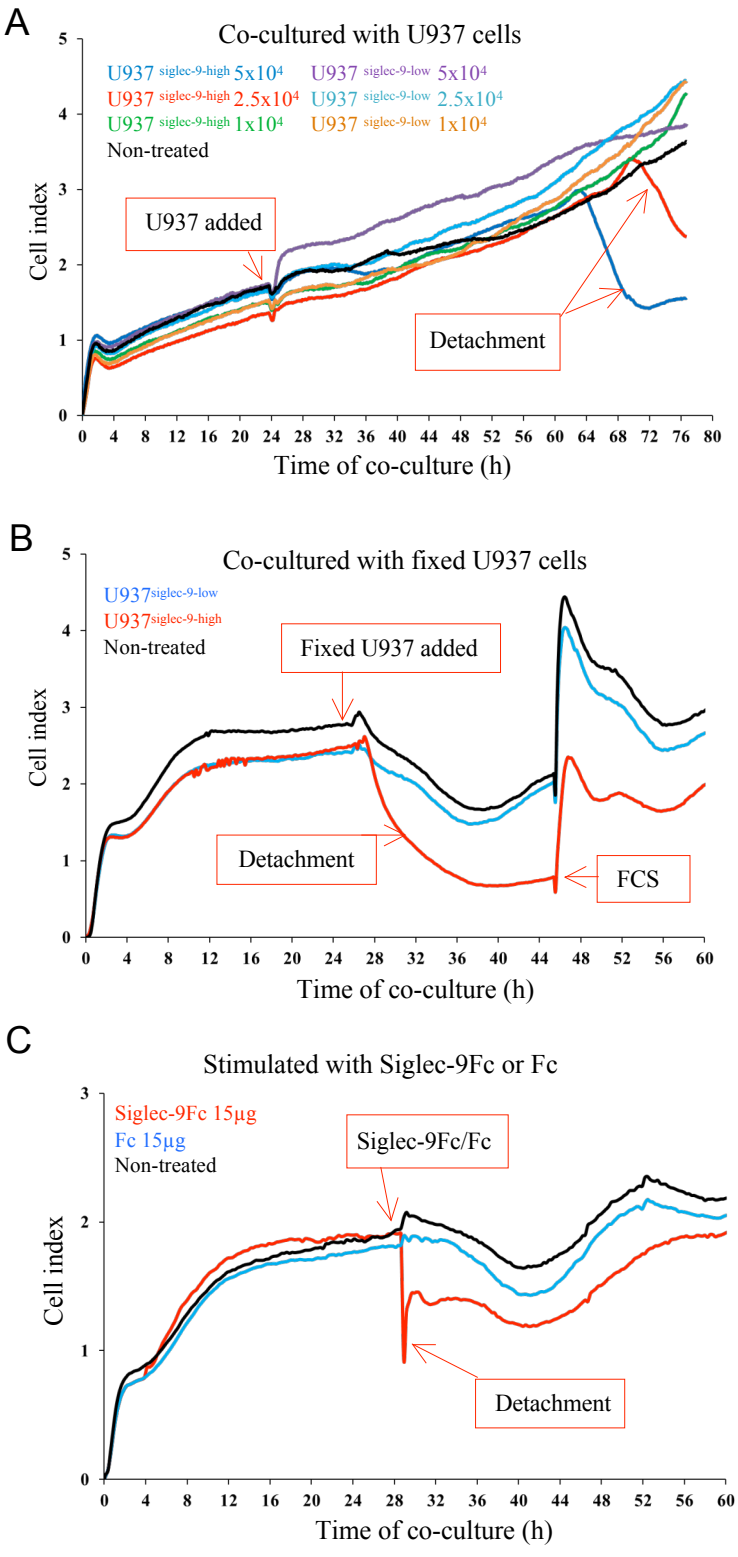
A
Co-cultured with U937 cells
U937 siglec-9-high 5x10⁴
U937 siglec-9-high 2.5x10⁴
U937 siglec-9-high 1x10⁴
U937 siglec-9-low 5x10⁴
U937 siglec-9-low 2.5x10⁴
U937 siglec-9-low 1x10⁴
Non-treated
U937 added
Detachment
Cell index
Time of co-culture (h)
B
Co-cultured with fixed U937 cells
U937siglec-9-low
U937siglec-9-high
Non-treated
Fixed U937 added
Detachment
FCS
Cell index
Time of co-culture (h)
C
Stimulated with Siglec-9Fc or Fc
Siglec-9Fc 15µg
Fc 15µg
Non-treated
Siglec-9Fc/Fc
Detachment
Cell index
Time of co-culture (h)

Fig. 3

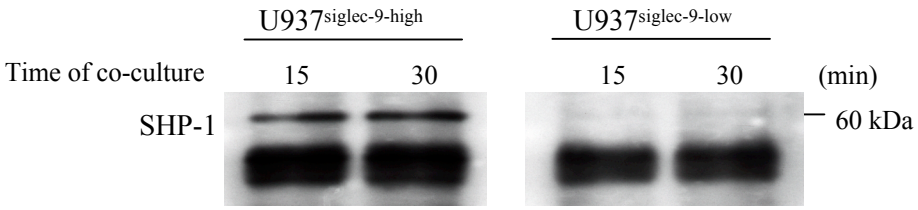
U937siglec-9-high
U937siglec-9-low
Time of co-culture
15
30
15
30
(min)
SHP-1
60 kDa

Fig. 4

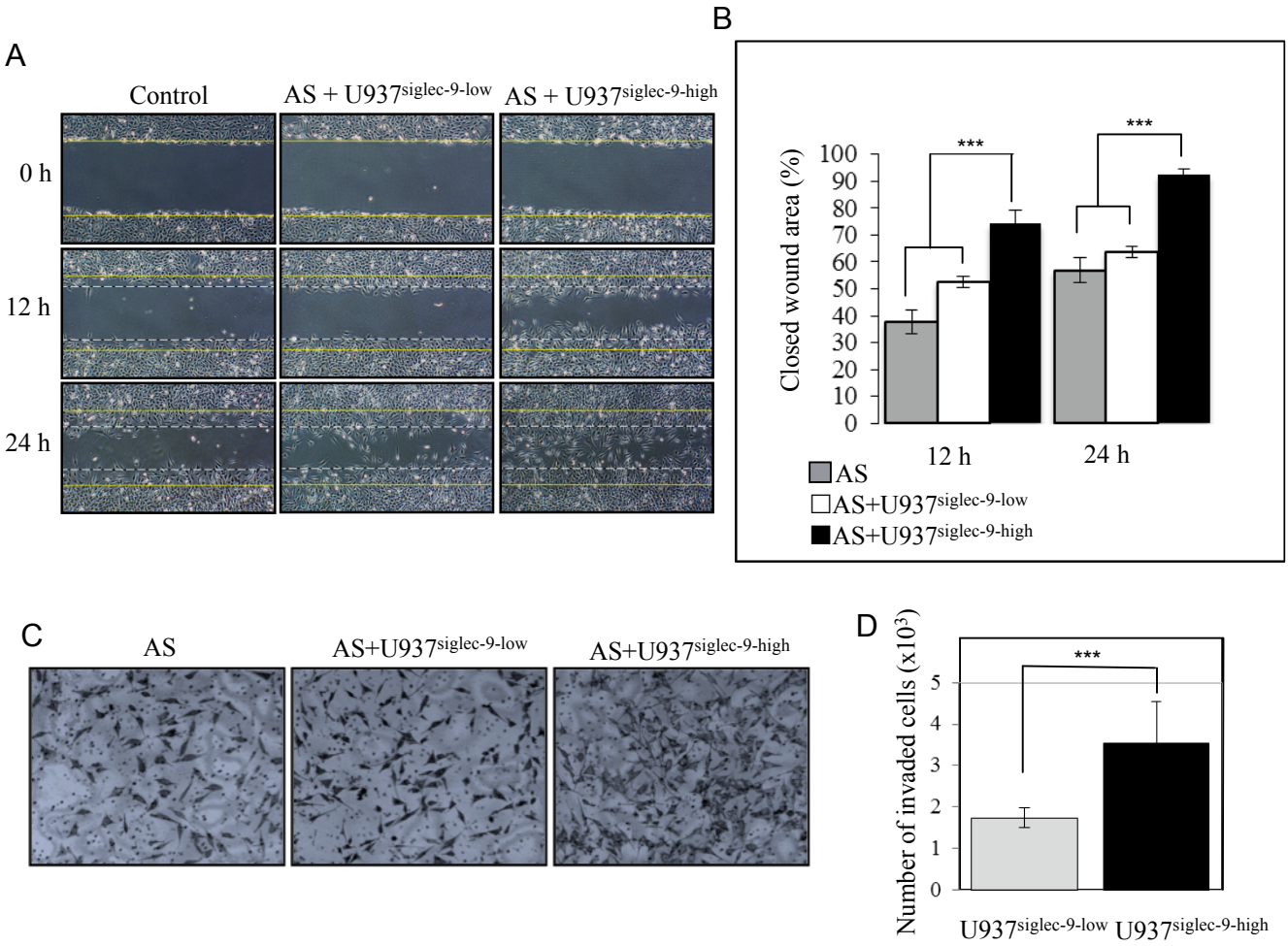
A
Control
AS + U937siglec-9-low
AS + U937siglec-9-high
0 h
12 h
24 h
B
Closed wound area (%)
100
90
80
70
60
50
40
30
20
10
0
***
***
12 h
24 h
AS
AS+U937siglec-9-low
AS+U937siglec-9-high
C
AS
AS+U937siglec-9-low
AS+U937siglec-9-high
D
Number of invaded cells (x10³)
5
4
3
2
1
0
***
U937siglec-9-low
U937siglec-9-high

Fig. 5

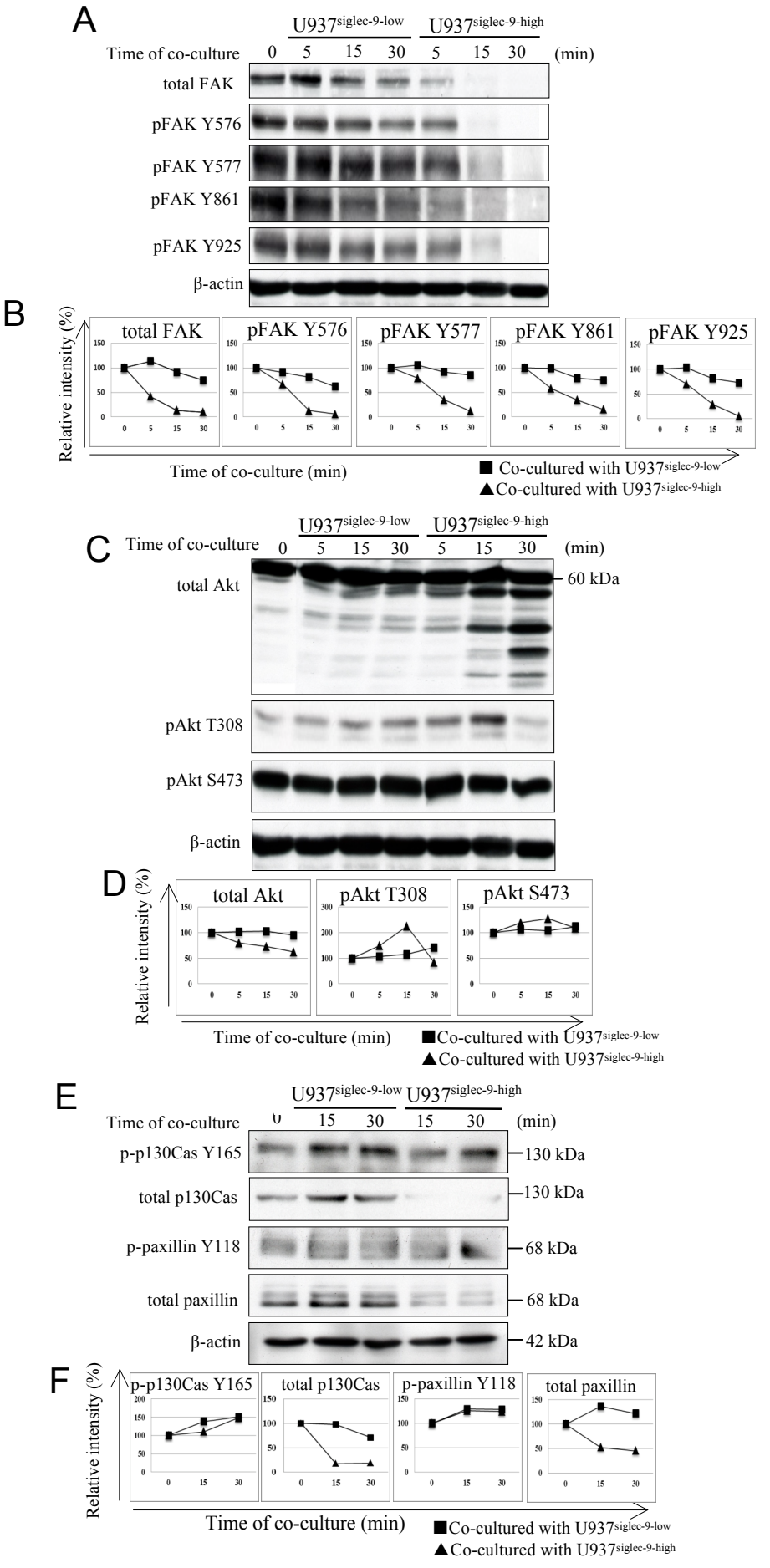
A
U937siglec-9-low
U937siglec-9-high
Time of co-culture
0 5 15 30 5 15 30 (min)
total FAK
pFAK Y576
pFAK Y577
pFAK Y861
pFAK Y925
β-actin
B
Relative intensity (%)
total FAK
pFAK Y576
pFAK Y577
pFAK Y861
pFAK Y925
Time of co-culture (min)
■ Co-cultured with U937siglec-9-low
▲Co-cultured with U937siglec-9-high
C
Time of co-culture
0 5 15 30 5 15 30 (min)
total Akt
60 kDa
pAkt T308
pAkt S473
β-actin
D
Relative intensity (%)
total Akt
pAkt T308
pAkt S473
Time of co-culture (min)
■Co-cultured with U937siglec-9-low
▲Co-cultured with U937siglec-9-high
E
Time of co-culture
0 15 30 15 30 (min)
p-p130Cas Y165
130 kDa
total p130Cas
130 kDa
p-paxillin Y118
68 kDa
total paxillin
68 kDa
β-actin
42 kDa
F
Relative intensity (%)
p-p130Cas Y165
total p130Cas
p-paxillin Y118
total paxillin
Time of co-culture (min)
■Co-cultured with U937siglec-9-low
▲Co-cultured with U937siglec-9-high

Fig. 6

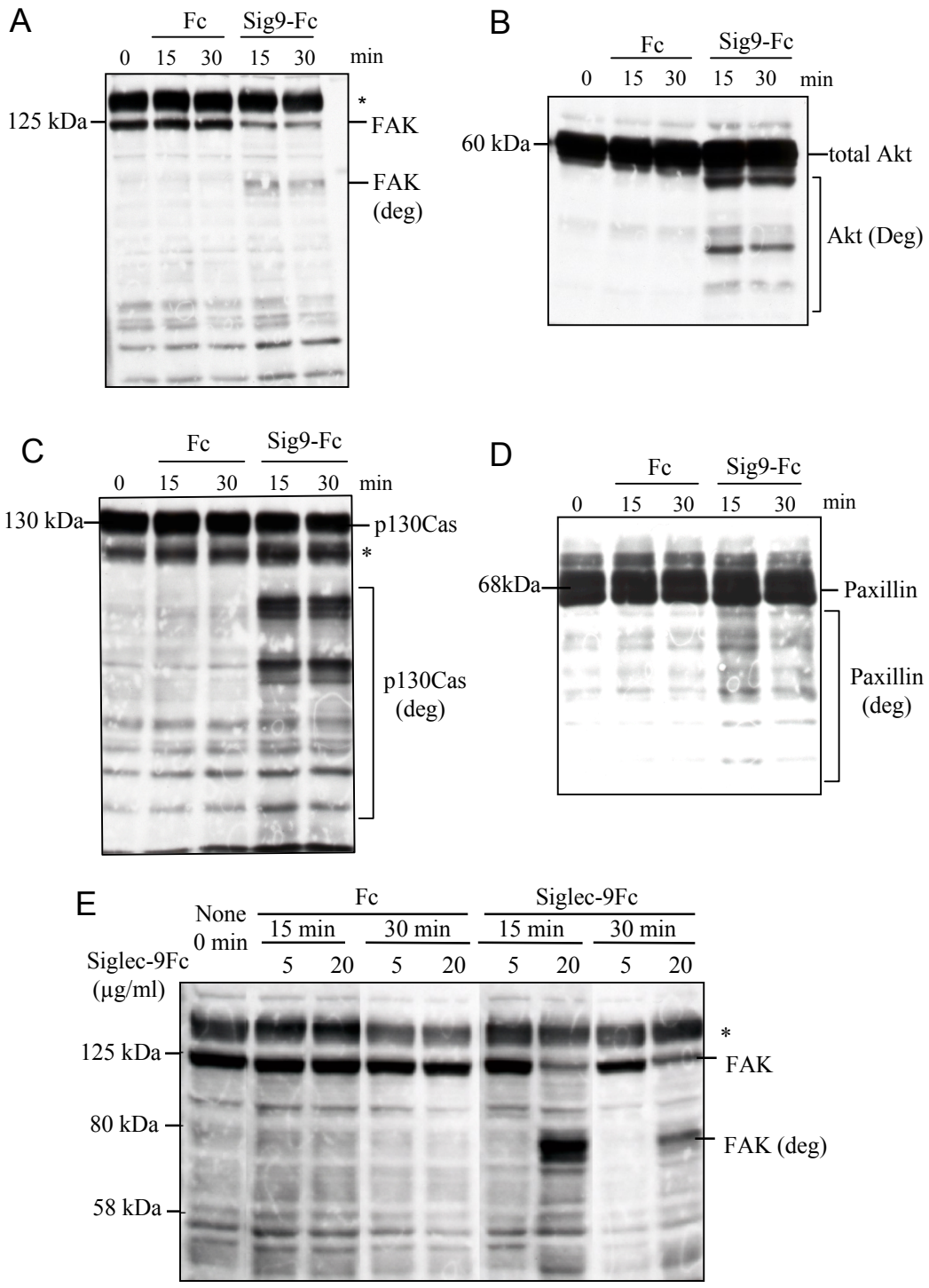
A
Fc
Sig9-Fc
0 15 30 15 30 min
125 kDa
*
FAK
FAK (deg)
B
Fc
Sig9-Fc
0 15 30 15 30 min
60 kDa
total Akt
Akt (Deg)
C
Fc
Sig9-Fc
0 15 30 15 30 min
130 kDa
p130Cas
*
p130Cas (deg)
D
Fc
Sig9-Fc
0 15 30 15 30 min
68kDa
Paxillin
Paxillin (deg)
E
None
0 min
Fc
Siglec-9Fc
15 min
30 min
15 min
30 min
Siglec-9Fc (µg/ml)
5 20 5 20 5 20 5 20
125 kDa
80 kDa
58 kDa
*
FAK
FAK (deg)

Fig. 7

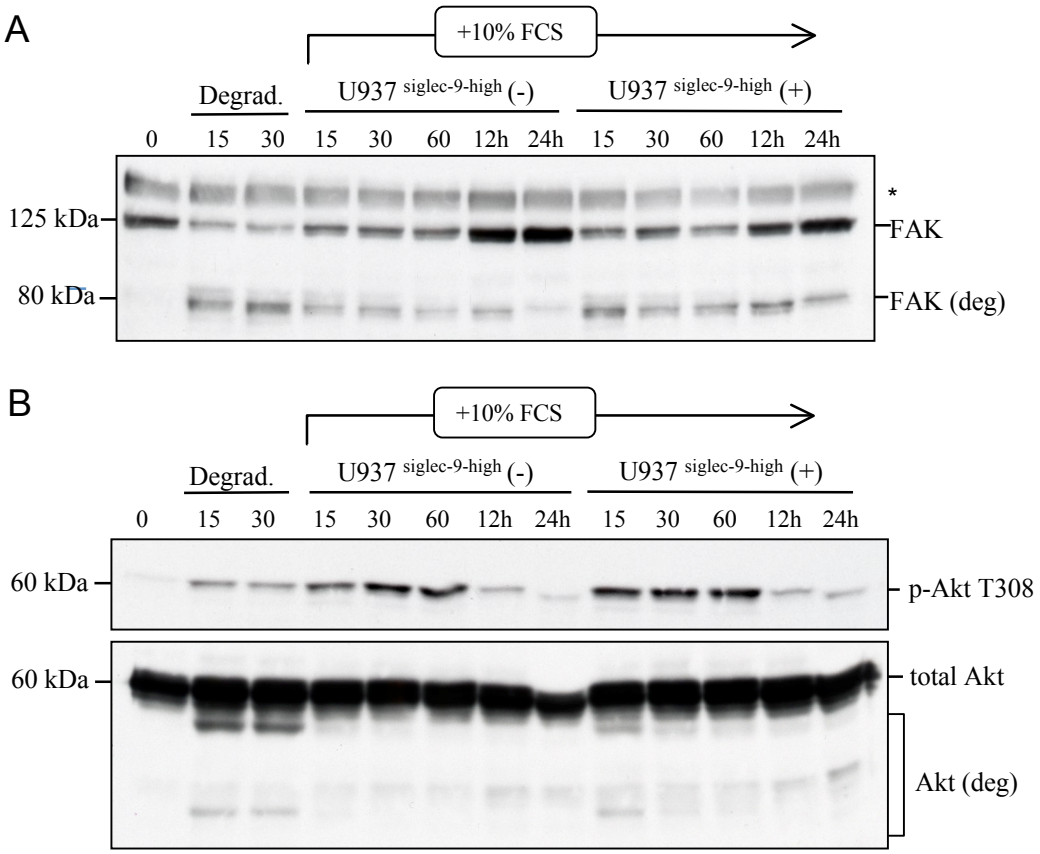
A
+10% FCS
Degrad.
U937 siglec-9-high (-)
U937 siglec-9-high (+)
0 15 30 15 30 60 12h 24h 15 30 60 12h 24h
125 kDa
80 kDa
*
FAK
FAK (deg)
B
+10% FCS
Degrad.
U937 siglec-9-high (-)
U937 siglec-9-high (+)
0 15 30 15 30 60 12h 24h 15 30 60 12h 24h
60 kDa
60 kDa
p-Akt T308
total Akt
Akt (deg)

Fig. 8

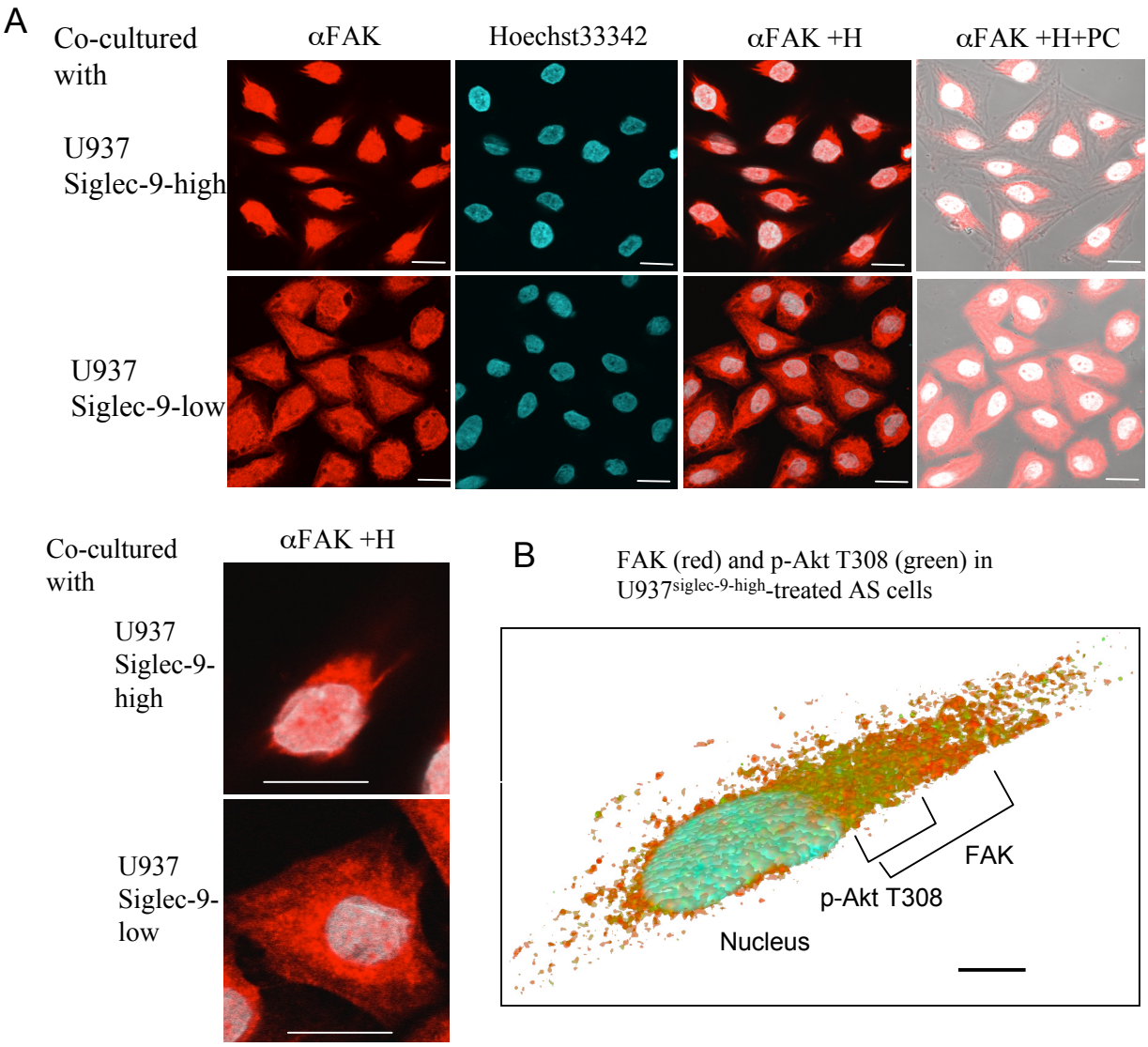
A
Co-cultured with
αFAK
Hoechst33342
αFAK +H
αFAK +H+PC
U937 Siglec-9-high
U937 Siglec-9-low
Co-cultured with
αFAK +H
U937 Siglec-9-high
U937 Siglec-9-low
B
FAK (red) and p-Akt T308 (green) in U937siglec-9-high-treated AS cells
FAK
p-Akt T308
Nucleus

Fig. 9

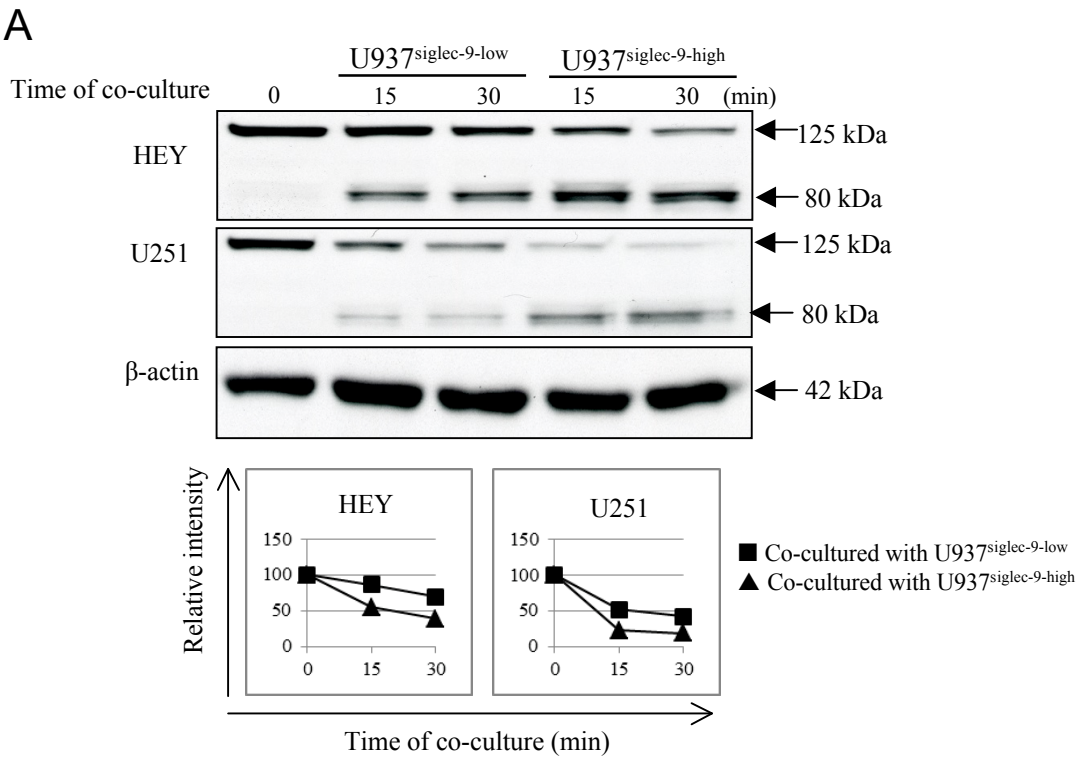
A
Time of co-culture
U937siglec-9-low
U937siglec-9-high
0
15
30
15
30
(min)
HEY
U251
β-actin
125 kDa
80 kDa
125 kDa
80 kDa
42 kDa
Relative intensity
HEY
U251
150
100
50
0
0
15
30
Co-cultured with U937siglec-9-low
Co-cultured with U937siglec-9-high
Time of co-culture (min)

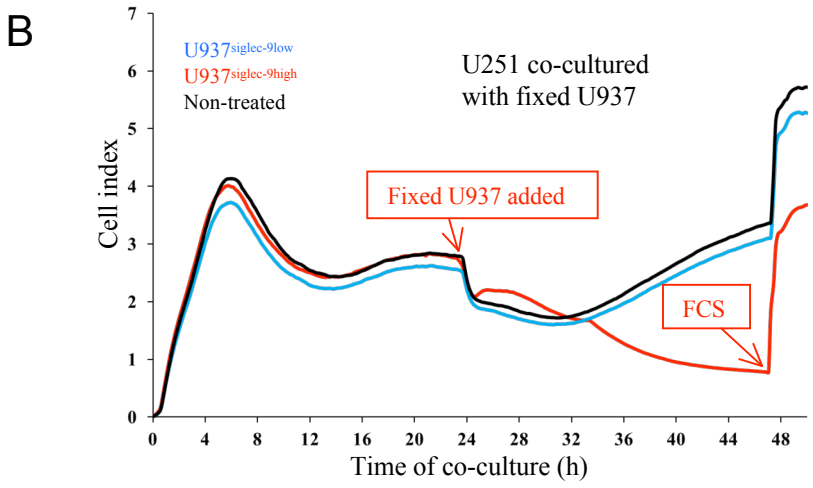
B
U937siglec-9low
U937siglec-9high
Non-treated
U251 co-cultured
with fixed U937
Fixed U937 added
FCS
Cell index
Time of co-culture (h)

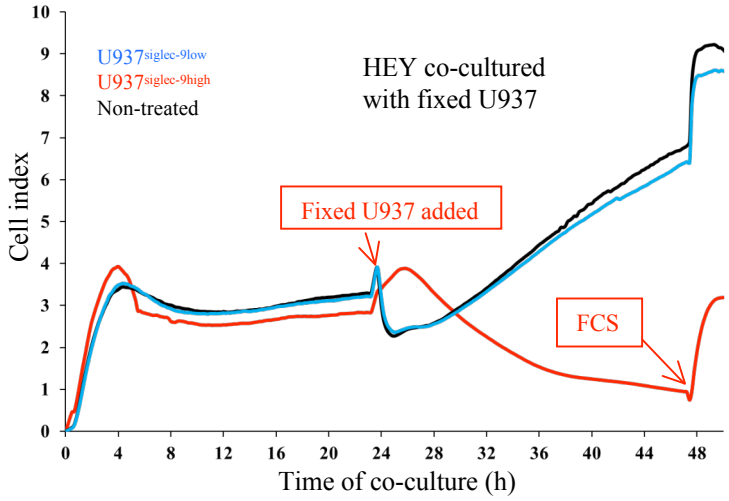
U937siglec-9low
U937siglec-9high
Non-treated
HEY co-cultured
with fixed U937
Fixed U937 added
FCS
Cell index
Time of co-culture (h)

Fig. 10

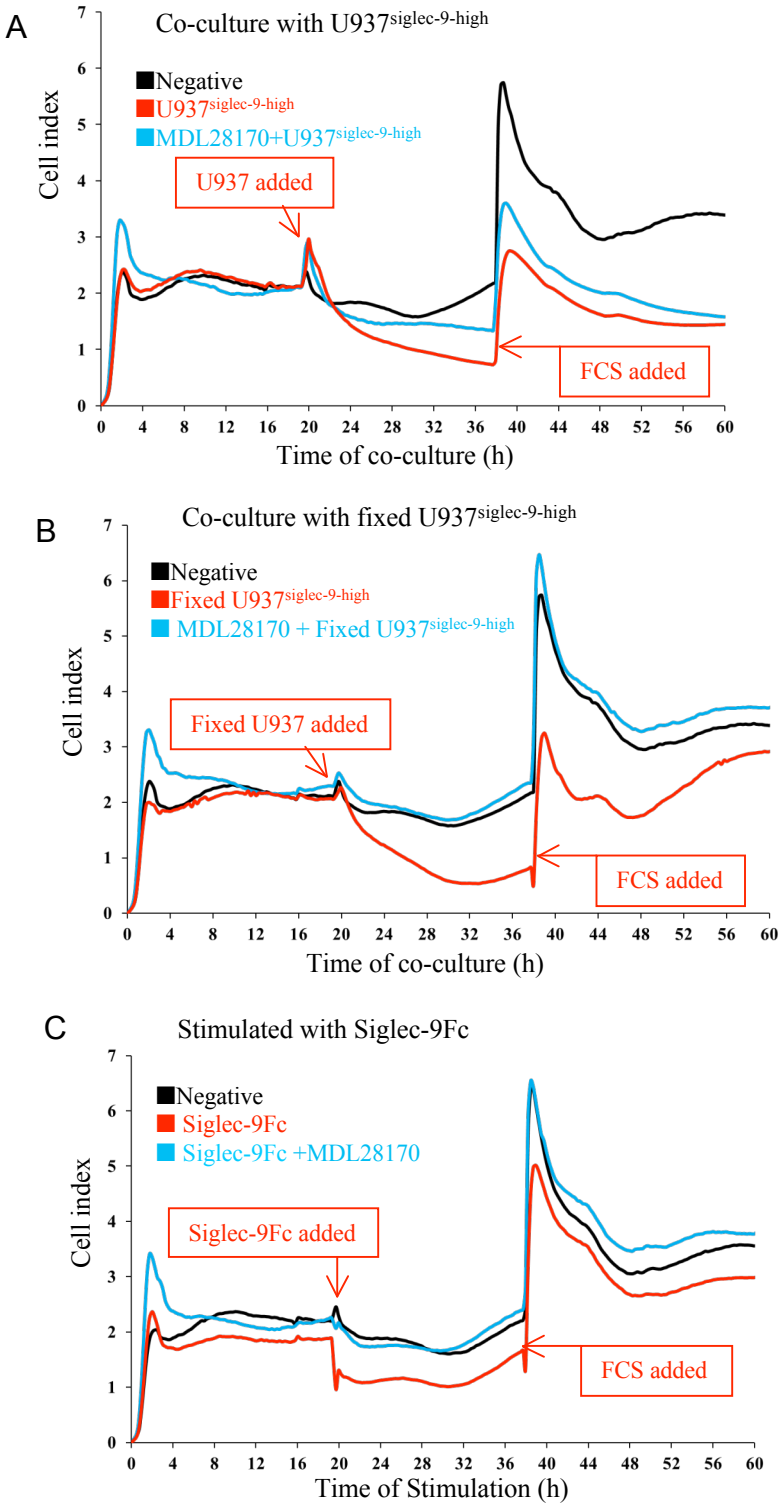
A
Co-culture with U937siglec-9-high
Negative
U937siglec-9-high
MDL28170+U937siglec-9-high
U937 added
FCS added
Cell index
Time of co-culture (h)
B
Co-culture with fixed U937siglec-9-high
Negative
Fixed U937siglec-9-high
MDL28170 + Fixed U937siglec-9-high
Fixed U937 added
FCS added
Cell index
Time of co-culture (h)
C
Stimulated with Siglec-9Fc
Negative
Siglec-9Fc
Siglec-9Fc +MDL28170
Siglec-9Fc added
FCS added
Cell index
Time of Stimulation (h)

Fig. 11

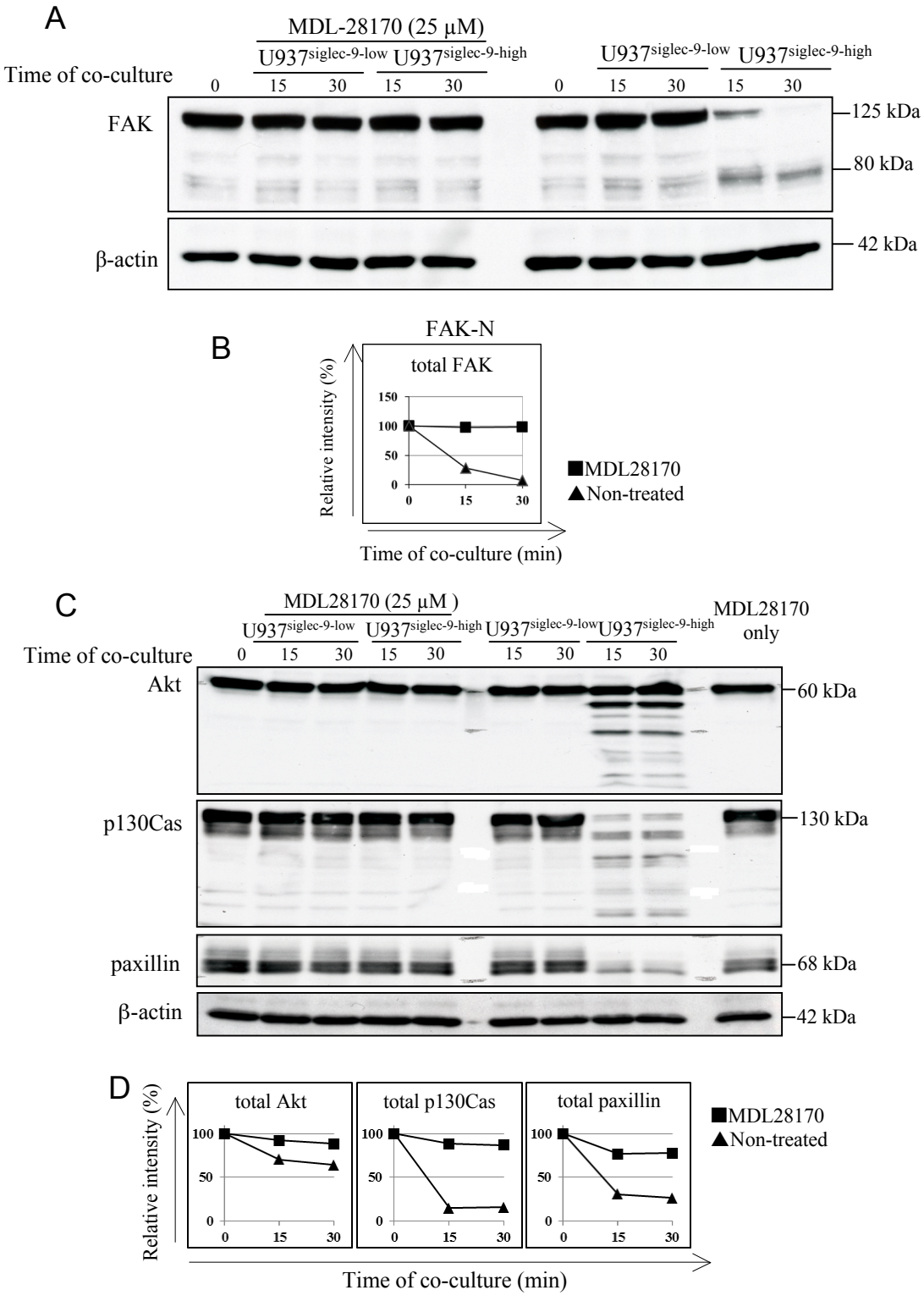
A
MDL-28170 (25 μM)
U937siglec-9-low
U937siglec-9-high
Time of co-culture
0
15
30
FAK
β-actin
125 kDa
80 kDa
42 kDa
B
FAK-N
total FAK
Relative intensity (%)
MDL28170
Non-treated
Time of co-culture (min)
C
MDL28170 (25 μM)
MDL28170 only
Akt
p130Cas
paxillin
β-actin
60 kDa
130 kDa
68 kDa
42 kDa
D
total Akt
total p130Cas
total paxillin
Relative intensity (%)
MDL28170
Non-treated
Time of co-culture (min)

Fig. 12

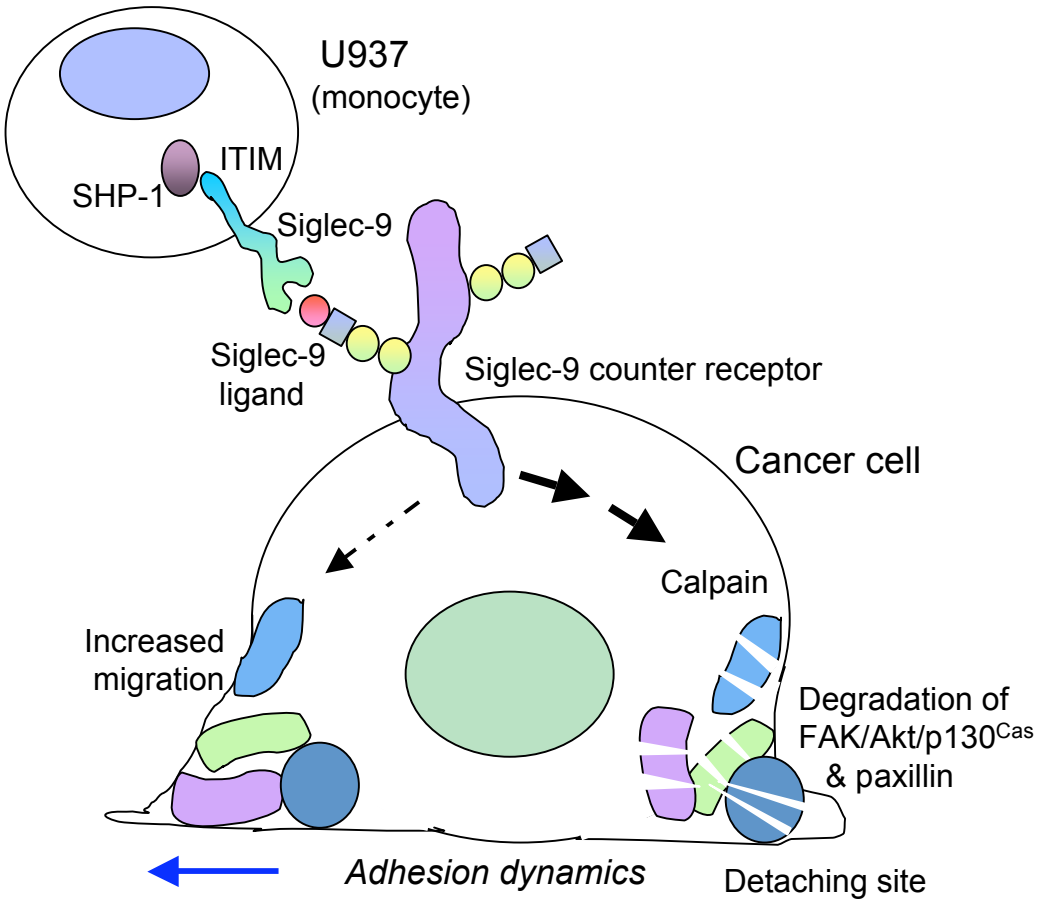
U937
(monocyte)
ITIM
SHP-1
Siglec-9
Siglec-9
ligand
Siglec-9 counter receptor
Cancer cell
Calpain
Increased
migration
Degradation of
FAK/Akt/p130Cas
& paxillin
Adhesion dynamics
Detaching site

Supplemental information

1. Supplemental Experimental Procedures.

2. Supplemental Table S1 and Table S2.

3. Supplemental Figures S1~S4, and Figure legends for Figure S1~Figure S4.

Supplemental Experimental Procedures:

Antibodies—Anti-β-actin (mouse mAb IgG1) was purchased from Sigma-Aldrich. Anti-c-Src (rabbit IgG, N-16) was from Santa Cruz Biotechnology, Inc. (Santa Cruz, CA). Anti-phospho-Src family kinases (Tyr-416, rabbit IgG), anti-Phospho-p44/42 MAPK (Erk1/2) (Thr202/Tyr204) (rabbit mAb IgG), anti-p44/42 MAPK (Erk1/2) (rabbit mAb IgG), and anti-cleaved caspase-3 (Asp175) (rabbit pAb IgG) antibodies were from Cell Signaling Technology, Inc. (Beverly, MA).

Flow cytometry of apoptosis—TACS^{TM} Annexin V-FITC apoptosis detection kit (Trevigent, Gaithersburg, MD) was used following the manufacturer's protocol.

Cell lines and culture—Human astrocytoma cell lines (5 lines), human acute leukemia cell lines (5 lines), human breast cancer cell line (3 lines), colon cancer cell lines (3 lines), human lung cancer cell lines (13 lines), human melanoma cell lines (8 lines), normal cell lines (2 lines), human neuroblastoma cell lines (2 lines), human ovarian cancer cell lines (11 lines), human renal cancer cell lines (20 lines), pancreatic carcinoma line (1 line), monocytic leukemia (1 line), and cervical cancer (1 line). All cell lines were maintained in Dulbecco's modified Eagle's medium (DMEM) (Sigma, St. Louis, MO) or RPMI1640 medium (Sigma) containing 10% FCS at 37 °C in 5 % CO_2. Siglec-9-over-expressing human histiocytic lymphoma (monocyte) U937$^{Siglec\text{-}9\text{-}high}$ cells and U937$^{Siglec\text{-}9\text{-}low}$ cells were generated as described (Ref. 10 in text), and both lines were maintained in the regular medium with G418 (450 μg/ml).

Immunoblotting—To examine signaling pathways in AS and other cell lines, cell lysates (15 μg) were separated by SDS-PAGE using 8% gels, and separated proteins were transferred onto a PVDF membrane (Millipore). Blots were blocked with 5% BSA in TBS containing 0.05% Tween-20 (TBST) for more than 6 h at 4°C. The membrane was first probed with primary antibodies. After being washed, the blots were then incubated with goat anti-rabbit IgGs or horse anti-mouse IgGs conjugated with HRP (1:2000). After washing, bound conjugates were visualized with an ECL^{TM} detection system (PerkinElmer). Band intensities were analyzed with Image J (NIH, http://rsbweb.nih.gov/ij/) and standardized with β-actin.

Supplemental Table S1. Results of flow cytometry to screen for binding of Siglec-9Fc to 75 human cell lines.

Cell type	Cell names	IMF
Glioma (n=5)	AS	344.47[1)]
	U87	96.78
	U251	141.3
	LN319	63.47
	T98	122.6
Acute leukemia (n=5)	Jurkat	102.55
	MT-1	40.52
	CCRF-CEM	3.71
	TS-1	99.36
	TS-2	109.25
Breast carcinoma (n=3)	MDA-MB-231	113.61
	MCF-7	99.23
	SK-BR-3	32.17
Colon carcinoma (n=3)	LoVo	46.99
	G3	27.72
	Caco-2	7.8
Lung carcinoma (n=13)	SK-LC-1	18.28
	SK-LC-10	347.12
	SK-LC-17	48.32
	SK-LC-33	290.83
	SA(ACC-LC-170)	23.35
	SM(ACC-LC-171)	66.45
	CALU-1	147.14
	YN	39.39
	QG90	138.73
	PC-10	101.42
	NCI-H69	26.62
	RERF-LC-MS(Mitsui cell)	22.82
	OKADA	201.32
Melanoma (n=8)	N1 GD3-	190.93

	N1 GD3+	132.89
	AU	116.39
	MEWO	74.27
	BD	72.35
	AOI	89.37
	SK-MEL-28	224.36
	KOHL-3	92
Normal cells (n=2)	HBEC4KT	32.86
	HEK-293T	71.06
Neuroblastoma (n=2)	IMR-32	62.21
	SK-N-SH	58.32
Ovarian carcinoma (n=11)	SAOV	145.75
	HRA	220.71
	HEY	271.04
	ES-2	188.4
	KOC-7C	32.59
	K2WT	64.17
	RMG-1	15.01
	RMG-2	62.89
	TOV21G	186
	OVCA3	10.06
	SCOV3	44.37
Renal cell carcinoma (n=20)	SK-RC-1	36.99
	SK-RC-6	49.85
	SK-RC-7	19.99
	SK-RC-17	49.29
	SK-RC-29	27.08
	SK-RC-35	57.48
	SK-RC-39	81.56
	SK-RC-44	36.72
	SK-RC-45	46.67
	SK-RC-99	54.06
	VMRC-RCZ	74.68

	VMRC-RCW	72.51
	OS-RC-2	43.04
	MOROFF	118.56
	CACI-1	45.24
	RCC-10RGB	36.05
	ACHN	7.11
	TUHR-4TKB	33.72
	TUHR-10TKB	0.78[2)]
	TUHR14TKB	83.51
Monocytic leukemia (n=1)	U937	42.86
Pancreatic carcinoma (n=1)	Capan-1	133.6
Cervical carcinoma (n=1)	Hela	105.1

[1)] Values are mean fluorescence intensity as compared with that of controls.

[2)] All of these cell lines were positive except TUHR-10TKB (MFI: 0.78).

Supplemental Table S2. Possible ligand carrier proteins recognized by Siglec-9Fc in LC/MS analysis

Protein name	Gene name	Subcellular location
Prostaglandin F2 receptor negative regulator	PTGFRN	Endoplasmic reticulum membrane; Single-pass type I membrane protein; Golgi apparatus, trans-Golgi network membrane
Integrin beta-1	ITGB1	Cell membrane; Single-pass type I membrane protein. Melanosome. Cleavage furrow.
Collectin-12	COLEC12	Membrane; Single-pass type II membrane protein.
ATP synthase subunit alpha, mitochondrial	ATP5A1	Mitochondrion inner membrane. Cell membrane; Peripheral membrane protein; Extracellular side
Endothelin-converting enzyme 1	ECE1	Cell membrane; Single-pass type II membrane protein.
Ig gamma-2 chain C region	IGHG2	Secreted.
Scavenger receptor class A member 3	SCARA3	Endoplasmic reticulum membrane; Single-pass type II membrane protein. Golgi apparatus membrane.
Galectin-3-binding protein	LGALS3BP	Secreted, extracellular space extracellular matrix
Integrin alpha-3	ITGA3	Membrane; Single-pass type I membrane protein.
Integrin alpha-5	ITGA5	Membrane; Single-pass type I membrane protein.
Cell surface glycoprotein MUC18	MCAM	Membrane; Single-pass type I membrane protein.
Serotransferrin	TF	Secreted.
DnaJ homolog subfamily A member 2	DNAJA2	Membrane; Lipid-anchor
HLA class I histocompatibility antigen, B-37 alpha chain	HLA-B	Membrane; Single-pass type I membrane protein.
HLA class I histocompatibility antigen, A-68 alpha chain	HLA-A	Membrane; Single-pass type I membrane protein.
Integrin alpha-6	ITGA6	Cell membrane; Single-pass type I membrane protein.
Integrin alpha-V	ITGAV	Membrane; Single-pass type I membrane protein.
HLA class I histocompatibility antigen, Cw-5 alpha chain	HLA-C	Membrane; Single-pass type I membrane protein.
Alpha-1,6-mannosylglycoprotein 6-beta-N-acetylglucosaminyltransferase B	MGAT5B	Golgi apparatus membrane; Single-pass type II membrane protein
Sodium/potassium-transporting ATPase subunit alpha-1	ATP1A1	Cell membrane; Multi-pass membrane protein. Melanosome.
Desmoglein-2	DSG2	Cell membrane; Single-pass type I membrane protein. Cell junction, desmosome.
HLA class I histocompatibility	HLA-A	Membrane; Single-pass type I membrane protein.

antigen, A-34 alpha chain		
EMILIN-1	EMILIN1	Secreted, extracellular space extracellular matrix.
HLA class I histocompatibility antigen, Cw-4 alpha chain	HLA-C	Membrane; Single-pass type I membrane protein.
Protocadherin gamma-C3	PCDHGC3	Cell membrane; Single-pass type I membrane protein
Cadherin-13	CDH13	Cell membrane; Lipid-anchor, GPI-anchor
Cadherin-11	CDH11	Cell membrane; Single-pass type I membrane protein.

To identify Siglec-9 ligand-carrier glycoproteins expressed on cancer cells, AS cell surface molecules were labeled with EZ-Link Sulfo-NHS-LC-Biotin, then precipitated with Siglec-9Fc. The bands in SDS-PAGE were digested and analyzed by LC-ESI-LIT-MS/MS. Under the identification threshold at 95% probability, totally 304 membrane or secreted proteins were identified in MS/MS. Consequently, twenty seven proteins in this table were classified as Siglec-9 specific molecules.

Figure Legends for Supplemental Figures:

Figure S1. Phenotypes of AS cells co-cultured with U937 cells. A, Representative image of AS cells cultured in plain RPMI1640 medium for 24 h (a), and co-cultured with U937$^{siglec\text{-}9\text{-}low}$ (b), or with U937$^{siglec\text{-}9\text{-}high}$ (c). (x100) After co-culture for 16 h in FCS-free condition, strong cell detachment was detected in AS cells co-cultured with U937$^{siglec\text{-}9\text{-}high}$ compared with those with negative controls. d, Re-attachment and rapid re-growth of AS cells after co-culture with U937 in the presence of 10% FCS for 24 h. B, No features of apoptosis were found in the detached AS cells co-cultured with U937$^{siglec\text{-}9\text{-}high}$ in immunoblotting of Caspase-3. No cleaved (activated) Caspase-3 was found in AS co-cultured with U937 cells. C, Flow cytometry to examine apoptosis induction. AS cells were seeded in 6-well plates at 1×10^5/well, and were cultured in the regular medium for 24 h at 37℃. Then, 5×10^5 of U937$^{siglec\text{-}9\text{-}high}$ or U937$^{siglec\text{-}9\text{-}low}$ cells in FCS-free RPMI1640 medium were added. After 16 h, cells were harvested by 2 mM EDTA/PBS. Cell apoptosis was analyzed by FACSCalibur (BD Bioscience) using TACS^{TM} Annexin V-FITC Kit (Trevigent) following the manufacturer's protocol. Contamination of U937 cells was avoided by gating small cell population in the FSC (forward scatter) and SSC (side scatter) dots (*left*). AS did not show apoptosis after co-culture with U937 cells for 16 h under FCS free condition. Higher levels of cell death were found rather in co-culture group with U937$^{siglec\text{-}9\text{-}low}$ (7% vs. 1.76%) (*right*). D, MTT assay of cell growth during co-culture. To examine the growth of AS cells co-cultured with U937$^{sigelc\text{-}9\text{-}high}$ or U937$^{siglec\text{-}9\ low}$ cells with various ratios as indicated in the figure. AS cells (2×10^3/100 μl/well) were seeded into 96-well plates and cultured in the regular medium for 24 h at 37 °C, then were co-cultured with U937 cells for 7 days. At every 24 h of co-culture, U937 cells were washed out by PBS, then 20 μl of MTT (5 mg/ml, Sigma) in PBS was added to each well. After incubation for 3.5 h at 37 °C, 150 μl of n-propyl alcohol containing 0.1% Nonidet P-40 and 4 mM HCl was added. The color reaction was quantitated using the automatic plate reader Immuno-Mini NJ-2300^{TM} (Nihon InterMed, Tokyo, Japan) at 590 nm with a reference filter of 620 nm. Triplicated samples were analyzed for one group. No significant differences in cell growth were shown during co-culture between AS cells co-cultured with U937$^{siglec\text{-}9\text{-}high}$ and those with U937$^{siglec\text{-}9\text{-}low}$.

Figure S2. ERK1/2 were activated almost equally in AS cells co-cultured with U937 cells. A, Immunoblotting of ERK1/2 and p-ERK1/2. AS cells were seeded into 6-well plates at

1×10^5/well, and cultured in the regular medium for 24 h at 37 °C. Then 1×10^6 U937$^{\text{siglec-9-high}}$ or U937$^{\text{siglec-9-low}}$ cells in FCS-free RPMI1640 medium were added. After co-culture for 15 and 30 min, cells were lyzed and 15 μl each of cell lysates was used for immunoblotting using anti-phospho-p44/42 MAPK (Erk1/2) (Thr202/Tyr204) and anti-p44/42 MAPK (Erk1/2) (Cell Signaling). Activation of Src was also examined under similar condition. B, Band intensities in Figure A were measured by ImageJ (http://rsb.info.nih.gov/ij/index.html) software, then statistical analysis was performed in Microsoft excel by correcting with bands of individual total proteins.

Figure S3. FAK degradation in AS cells during co-culture with U937$^{\text{siglec-9-high}}$ was prevented by pre-treatment with sialidase. AS cells were treated for 2 h by 100 mU/ml sialidase as shown in Fig. S1, and were used for co-culture experiments with U937$^{\text{siglec-9-high}}$ as described in Fig. 2. Immunoblotting with anti-FAK was also performed as described in Fig. 2.

Figure S4. Spatial dynamics of FAK and p-Akt during co-culture of AS cells with U937. Six x10^4 AS in 2ml of 10% FCS-containing RPMI1640 were seeded in glass-based dishes (Iwaki, Japan), and cultured for 24 h, then FCS was starved for 12 h. Then AS cells were co-cultured with 1x10^6/dish of U937$^{\text{siglec-9-high}}$ or U937$^{\text{siglec-9-low}}$ cells. U937 cells were removed after co-culture for 15 and 30 min, then cells were fixed with 4% paraformaldehyde/PBS for 10 min at room temperature, and permeabilized with 0.1% Triton X-100/PBS for 5 min. After being blocked with 5% BSA/PBS for 60 min, cells were stained with anti-FAK antibody (mouse IgG, BD Biosciences; at 1:400 dilution), or anti-p-Akt T308 (rabbit IgG, Cell signaling; at 1:400 dilution) for 60 min, and stained with 1:400 dilution of Alexa Fluor 555-goat anti-mouse IgG1 (Invitrogen, 1:400 dilution) for FAK or Alexa Fluor 488-goat anti-rabbit IgG (H+L) antibody (Invitrogen) for p-Akt T308 for 60 min in the dark. Finally cells were stained with 1:10,000 dilution of Hoechst 33342 (Invitrogen) for nucleus for 15 min in the dark.

Immunofluorescence signal of cells was observed with confocal laser scanning biological microscope FV10i, photographed under 108 x zoom, scanned by XYZ mode with 0.2 μm/slice for 50 μm depth (Z),118 x 118 μm (X x Y) of area, and analyzed by Fluoview FW10-ASW software (ver 3.01) for 3-dimensional imaging. Channel 1 set to nucleus (cyan), channel 2 set to p-Akt T308 (green) (E, F), channel 3 set to FAK (red) (C, D, overlapped with nucleus) and channel 4 set to phase contrast images (A, B). A, C, E, G are of AS cells co-cultured with U937$^{\text{siglec-9-high}}$ (scale bars, 10 μm), and B, D, F, H are of those co-cultured with U937$^{\text{siglec-9-low}}$

(scale bars, 8 μm).

Fig. S1

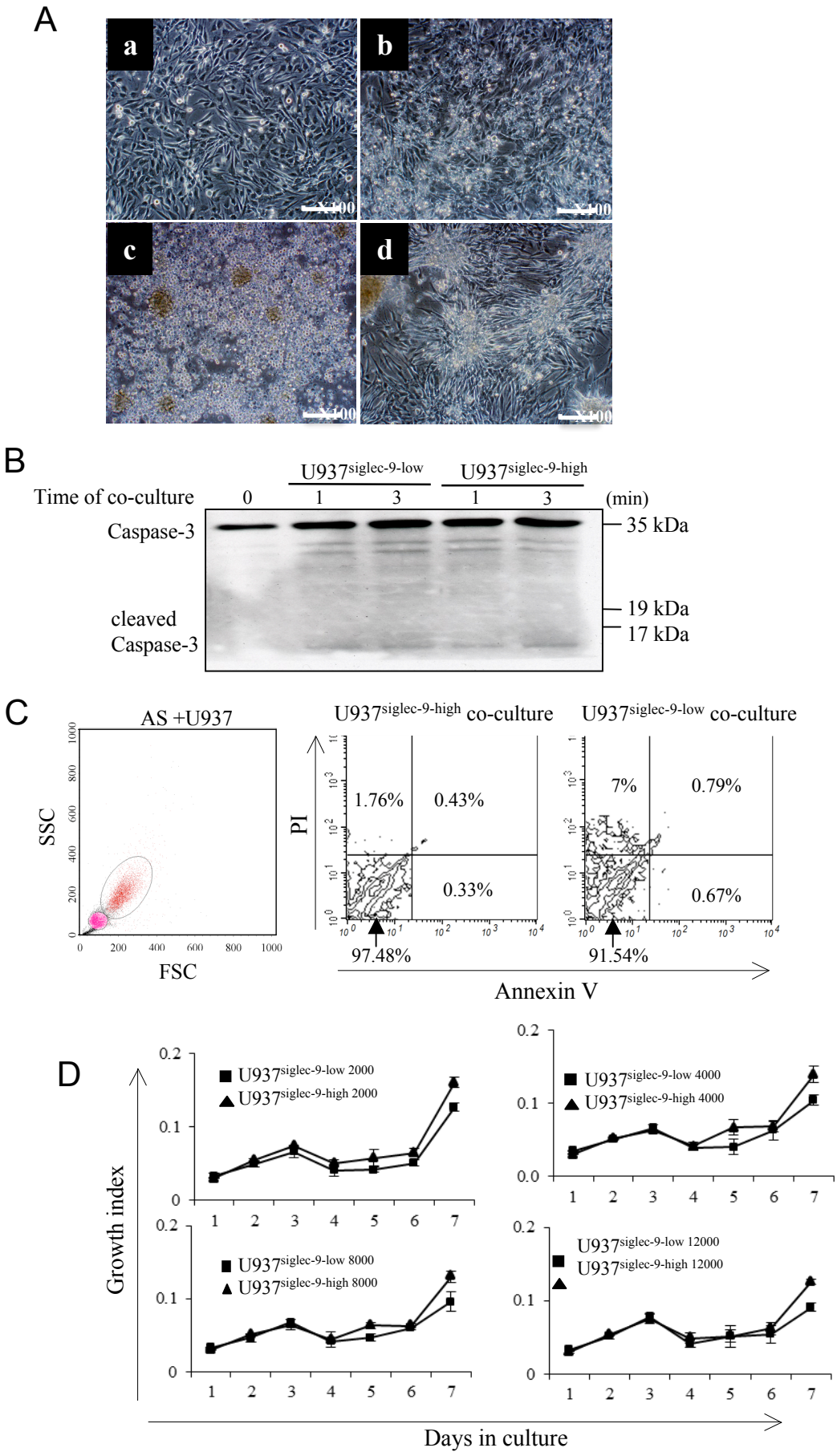
A
a
b
c
d
B
U937siglec-9-low
U937siglec-9-high
Time of co-culture
0
1
3
1
3
(min)
Caspase-3
35 kDa
cleaved
Caspase-3
19 kDa
17 kDa
C
AS +U937
SSC
FSC
U937siglec-9-high co-culture
U937siglec-9-low co-culture
PI
1.76%
0.43%
0.33%
97.48%
7%
0.79%
0.67%
91.54%
Annexin V
D
U937siglec-9-low 2000
U937siglec-9-high 2000
U937siglec-9-low 4000
U937siglec-9-high 4000
U937siglec-9-low 8000
U937siglec-9-high 8000
U937siglec-9-low 12000
U937siglec-9-high 12000
Growth index
Days in culture

Fig. S2

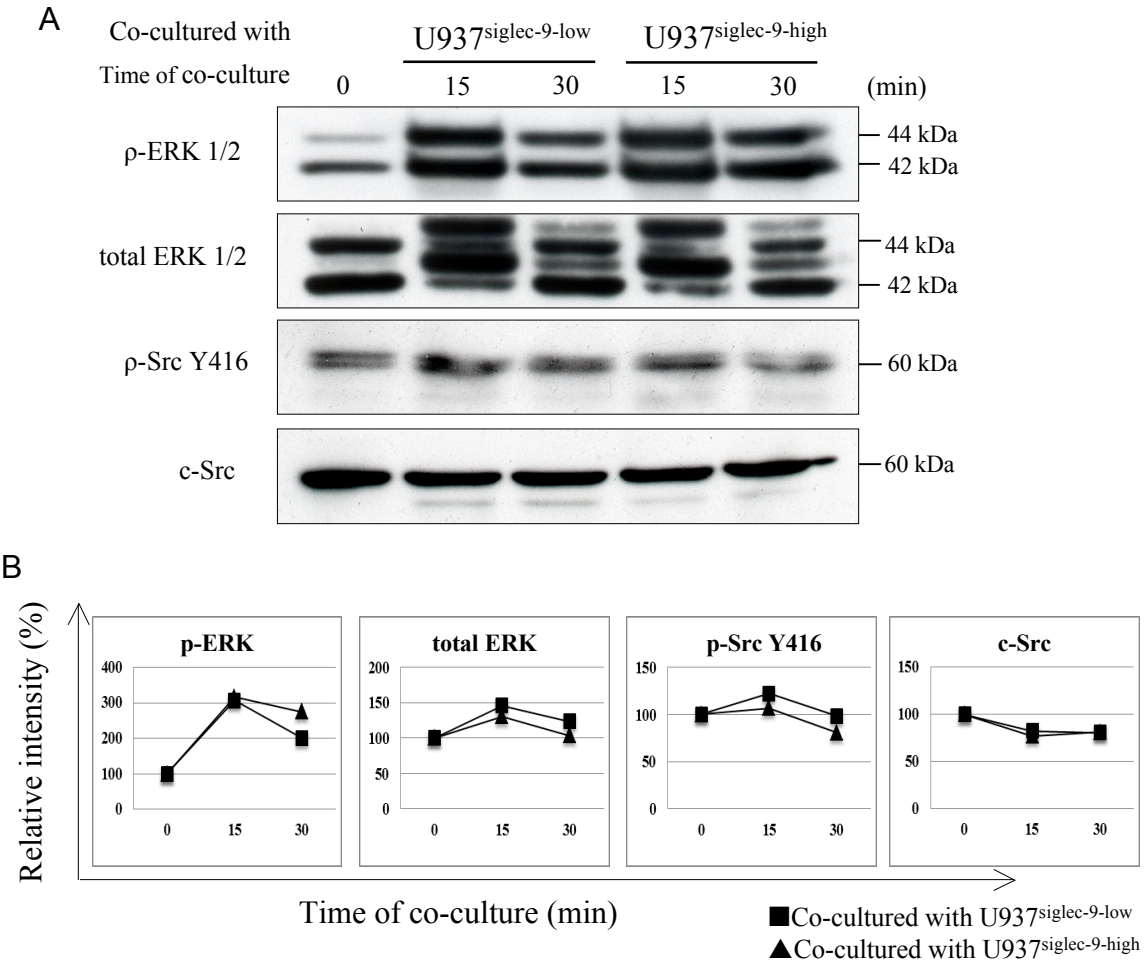
A
Co-cultured with
U937siglec-9-low
U937siglec-9-high
Time of co-culture
0
15
30
15
30
(min)
ρ-ERK 1/2
44 kDa
42 kDa
total ERK 1/2
44 kDa
42 kDa
ρ-Src Y416
60 kDa
c-Src
60 kDa
B
Relative intensity (%)
p-ERK
total ERK
p-Src Y416
c-Src
Time of co-culture (min)
■Co-cultured with U937siglec-9-low
▲Co-cultured with U937siglec-9-high

Fig. S3

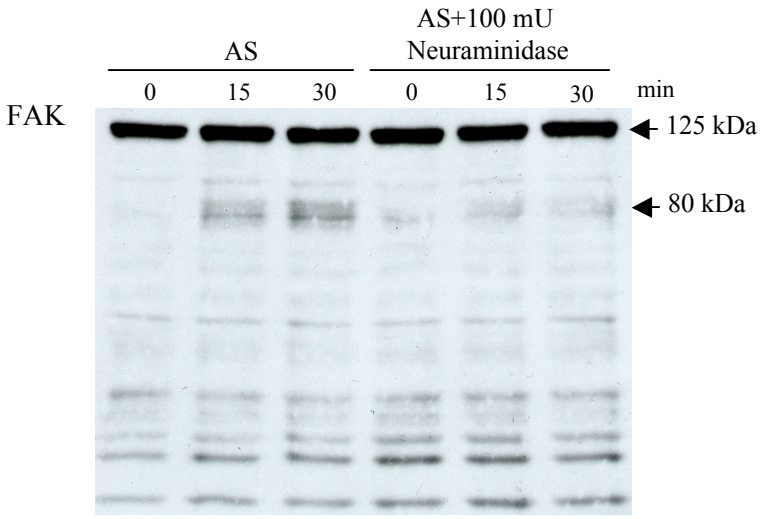

Fig. S4